https://doi.org/10.5194/egusphere-2026-2720
Preprint. Discussion started: 29 May 2026

High-resolution reconstruction of pH upregulation and its seasonal drivers in the temperate coral *Cladocora caespitosa*

Marina J. Vergotti[1], Diego K. Kersting[2], Thomas C. Brachert[3], Steeve Comeau[4], Daniel A. Frick[5,6], Ed C. Hathorne[7], Michael J. Henehan[5,8], Josefine Holtz[5], Núria Teixidó[4,9], Valby van Schijndel[10], and Juan Pablo D'Olivo[11]

[1]Department of Palaeontology, Institute of Geological Sciences, Freie Universität Berlin, Berlin 12249, Germany
[2]Institute of Aquiculture Torre de la Sal, Spanish National Research Council (CSIC), Ribera de Cabanes 12595, Spain
[3]Institute of Earth System Research and Remote Sensing, University of Leipzig, Leipzig 04103, Germany
[4]Laboratory of Oceanography of Villefranche (LOV-CNRS), Sorbonne University, Villefranche-sur-Mer 06230, France
[5]Section 3.2 Organic and Earth Surface Geochemistry, GFZ Helmholtz Centre for Geosciences, Potsdam 14473, Germany
[6]Paleoceanography and Marine Geology, Institute of Geosciences, Kiel University, Kiel 24118, Germany
[7]Department of Ocean Circulation and Climate Dynamic, GEOMAR Helmholtz Centre for Ocean Research, Kiel 24148, Germany
[8]School of Earth Sciences, University of Bristol, Bristol BS8 1QU, United Kingdom
[9]Stazione Zoologica Anton Dohrn- National Institute of Marine Biology, Ecology and Biotechnology, Ischia Marine Centre, Ischia 80077, Italy
[10]Section 3.1 Inorganic and Isotope Geochemistry, GFZ Helmholtz Center for Geosciences, Potsdam 14473, Germany
[11]Unidad Académica de Sistemas Arrecifales, Instituto de Ciencias del Mar y Limnología, Universidad Nacional Autónoma de México, Puerto Morelos 77580, Mexico

Correspondence to: Marina J. Vergotti (mj.vergotti@gmail.com)

Abstract. Ocean acidification (OA) and associated changes in seawater carbonate chemistry, combined with thermal stress, hampers coral calcification. By upregulating pH and dissolved inorganic carbon, corals can optimize their calcification, giving them some resilience to OA. Little is known about the seasonal- and interannual scale impacts of thermal stress and OA on pH upregulation and calcification in the temperate coral *Cladocora caespitosa*, despite it being the only zooxanthellate reef builder in the Mediterranean Sea. $\delta^{11}B$ and B/Ca were determined seasonally in *C. caespitosa* skeletons from two NW Mediterranean sites to reconstruct the effect of seawater temperature and pH on the carbonate chemistry of the coral calcifying fluid (CF), at a bimonthly resolution from June 2013 to August 2017 (Columbretes Islands, Spain), and June 2016 to February 2022 (Villefranche-sur-Mer, France). *Cladocora caespitosa* displayed a similar pH upregulation strategy to most tropical corals, albeit with an apparently lower sensitivity to seasonal environmental change. Temperature was the main driver of seasonal variability in the CF composition and coral calcification, with seawater pH having a comparatively lower seasonal variability, and acting on longer timescales. While longer coral records and investigations into inter-population variability would still be beneficial in order to fully understand the response of *C. caespitosa* to environmental change, our records constitute an important first step in understanding the biomineralization strategy of this ecologically important coral species.

https://doi.org/10.5194/egusphere-2026-2720
Preprint. Discussion started: 29 May 2026

1 Introduction

Ocean warming and acidification threaten marine calcifiers worldwide (IPCC, 2019). Ocean acidification (OA) has already caused a decline in pH of more than 0.1 pH units relative to pre-industrial levels and is projected to decrease a further 0.4 pH units by 2100 (IPCC, 2019; Kwiatkowski et al., 2020). As a result of the decline in pH, dissolved inorganic carbon (DIC) species shift towards a higher concentration of dissolved CO_2 and bicarbonate (HCO_3^-), and a lower concentration of carbonate ion (CO_3^{2-}). This shift results in a decrease in the saturation state (Ω) of calcium carbonate ($CaCO_3$) in seawater, the building block for marine calcifiers such as corals (Gattuso et al., 1999, 2015a; Kleypas et al., 2006; Pandolfi et al., 2011). The combined long-term effects of warming and OA on calcifiers like corals are still only partially understood. Limitations arise from the spatially and temporally constrained records of ocean pH and carbonate chemistry, combined with the lack of information on ecosystem- and community-level responses. Corals, as some of the longest-lived marine calcifiers, are valuable long-term recorders of environmental information, as well as indicators of individual organisms' responses to warming and OA (Chen et al., 2019; D'Olivo et al., 2019a; Fowell et al., 2018; Kang et al., 2024; McCulloch et al., 2017). Although coral records have been most commonly generated from tropical oceans, they have also proven valuable for understanding environmental change in temperate regions such as the Mediterranean Sea (Kersting et al., 2025; Montagna et al., 2007; Royle et al., 2015b, a; Vergotti et al., 2025b).

The Mediterranean Sea is a climate change hot-spot, with warming rates ~20 % higher than the global average (Garrabou et al., 2022; Hassoun et al., 2025; IPCC, 2019; Martínez et al., 2023). With its high levels of alkalinity, worst-case-scenarios climatic projections indicate rates of OA higher than the global average, with current rates of approximately -0.003 units·yr^{-1} (Geri et al., 2014; Hassoun et al., 2025). The Mediterranean Sea is also characterized by its marked seasonality with winters characterized by low temperatures and levels of irradiance, and high vertical mixing while high summer temperatures drive water column stratification and nutrient depletion in the surface ocean (Coma et al., 2009). This combination of rapid warming, high alkalinity, and marked seasonality results in a unique setting to investigate coral responses to climate change.

Cladocora caespitosa, an endemic Mediterranean scleractinian coral, is a key bioengineering species and the sole potential reef-builder coral in this region (Kersting and Linares, 2012; Kružić and Benković, 2008; Peirano et al., 1998, 2001; Pitacco et al., 2017). Well adapted to the high seasonality of the Mediterranean, *C. caespitosa* has a high habitat plasticity, thriving in both well-lit and dim-light environments, thus often occurring in shallow-photophilic communities within algal assemblages, and deeper, in mesophotic communities, up to 50 m deep (Hoogenboom et al., 2010; Kersting et al., 2015, 2017, 2023; Morri et al., 1994; Pons-Fita et al., 2021; Schiller, 1993). Nevertheless, warming and reoccurring marine heatwaves (MHW) have repeatedly impacted this species both at lethal and sub-lethal levels (Kersting et al., 2013; Vergotti et al., 2025b), leading to its classification as and "endangered" species in the International Union for the Conservation of Nature (IUCN) red-list since 2015 (Casado-Amezúa et al., 2015; Kersting et al., 2022). Past variations of *C. caespitosa* skeletal growth rate have been

https://doi.org/10.5194/egusphere-2026-2720
Preprint. Discussion started: 29 May 2026

related to temperature changes (Kružić et al., 2012; Morri et al., 1994; Vergotti et al., 2025b), and high-resolution temperature reconstructions using geochemical proxies (Kersting et al., 2025; Montagna et al., 2007; Royle et al., 2015b; Silenzi et al., 2005), clearly highlight the potential of *C. caespitosa* as a paleo-climate recorder of environmental conditions for the Mediterranean Sea.

High resolution reconstructions of geochemical proxies in coral skeletons can help us bridge some of these knowledge gaps. Among them, boron isotopes are a well-established proxy for seawater pH (pH_{sw}) (Foster and Rae, 2016; Hemming and Hanson, 1992; Vengosh et al., 1991). Corals, however, complicate this relationship as they physiologically control the composition of their calcifying fluid (CF) by elevating their internal pH (pH_{cf}) with respect to seawater. This "vital effect", commonly referred to as "pH upregulation", allows corals to set optimal conditions for the precipitation of their skeleton (McCulloch et al., 2012; Trotter et al., 2011; Venn et al., 2013). The upregulation of pH_{cf} shifts the equilibrium of the DIC_{cf} species towards CO_3^{2-}, increasing the aragonite saturation state (Ω_{cf}) and promoting the precipitation of $CaCO_3$ (Al-Horani et al., 2003; Cohen and McConnaughey, 2003; McCulloch et al., 2017). The degree of pH upregulation can be accounted for when reconstructing changes in pH_{sw} from $\delta^{11}B$ via species-specific $\delta 11B_{carb}$-pH calibration curves (Holcomb et al., 2014; Hönisch et al., 2004; Krief et al., 2010; Trotter et al., 2011).

Studies on coral pH upregulation to date have focused on tropical corals, reporting seasonal, and even multi-decadal oscillations of pH_{cf} modulated by pH_{sw} and indirectly by temperature, irradiance, and water flow, with a concomitant decrease of pH_{cf} in response to the global OA trend (Comeau et al., 2017a, 2019a; D'Olivo et al., 2019a; Kang et al., 2024; McCulloch et al., 2017). Further, environmental stress such as long-term warming and MHWs can disrupt pH upregulation, causing a loss of seasonal cycles in pH_{cf}, and sometimes altering growth rates (D'Olivo et al., 2019a; D'Olivo and McCulloch, 2017; Wei et al., 2009), underlining the importance of pH upregulation for calcification. Upregulation was described by Trotter et al. (2011) for the first time in *C. caespitosa*, showing that while the pH_{cf} decreased under acidified conditions, the upregulation of pH_{cf} relative to pH_{sw} was in fact increased. Nevertheless, comparatively to tropical corals fewer studies have been conducted in the Mediterranean Sea, with most studies investigating the calcification response of *C. caespitosa* to OA involving mainly short-term *aquaria* experiments with contrasting results. In some such studies, no apparent changes in calcification rates were found in response to acidified conditions, an outcome attributed to the lower carbonate requirements arising from the lower growth rates of *C. caespitosa* (Carbonne et al., 2021; Rodolfo-Metalpa et al., 2010). Contrastingly, decreasing calcification rates were observed when experimentally combining acidified conditions with low food availability (Movilla et al., 2012), highlighting the need of energetic input to sustain pH upregulation when corals are exposed to combined stressors. In another study evaluating differences between *C. caespitosa* colonies grown across a natural pH gradient at a hydrothermal vent site, Hulver et al. (2025) suggested that coral growth was maintained under acidified conditions thanks to a higher heterotrophic capacity. As such, the effect of OA and other environmental factors on the calcification process of *C. caespitosa*, particularly at the sub-

https://doi.org/10.5194/egusphere-2026-2720
Preprint. Discussion started: 29 May 2026

annual scale, remains only partially understood, and to date, no high-resolution reconstruction of the pH upregulation of *C. caespitosa* has been attempted.

In this study, we produce, for the first time, high-resolution records of seasonal and interannual variations in the pH_{cf} of *C. caespitosa* from two sites of the NW Mediterranean with distinct temperature patterns. We aim to understand how different environmental parameters affect coral pH upregulation and calcification. Understanding the environmental drivers of coral calcification, and how temperate corals growth varies under seasonally and interannually changing environmental conditions is paramount to predict their future response to climate change.

2 Methods

2.1 Coral sampling

A fragment consisting of 10 to 20 corallites was collected from a single living colony of the coral *C. caespitosa* in two locations of the NW Mediterranean Sea (Fig. 1). The fragments were collected at 15 m depth in August 2017, in the Columbretes Islands (39°53.825' N, 0°41.214' E, Spain), and at 10 - 15 m depth in February 2022, in the bay of Villefranche-sur-Mer (43°68.960' N, 7°30.836' E, France). The fragments were subsequently cleaned of organic material and sediment in a 1:1 NaOCl and deionized water bath (Vergotti et al., 2025b) before selecting and separating the longest and straightest individual corallites, with the least bioerosion marks. Three corallites were selected from the colony fragment collected in Villefranche (labelled V3-1, V3-2, and V3-3), and four corallites from the fragments collected in the Columbretes Islands (labelled C3-1, C3-2, C3-3, and C3 7) (Fig. B1). Sample C3-7 was previously analysed for $\delta^{18}O$ and $\delta^{13}C$ (Kersting et al., 2025). The selected corallites were X-rayed to measure coral growth and establish a preliminary chronology. Specific methods for sample cleaning and X-raying are outlined in detail in Vergotti et al. (2025).

https://doi.org/10.5194/egusphere-2026-2720
Preprint. Discussion started: 29 May 2026

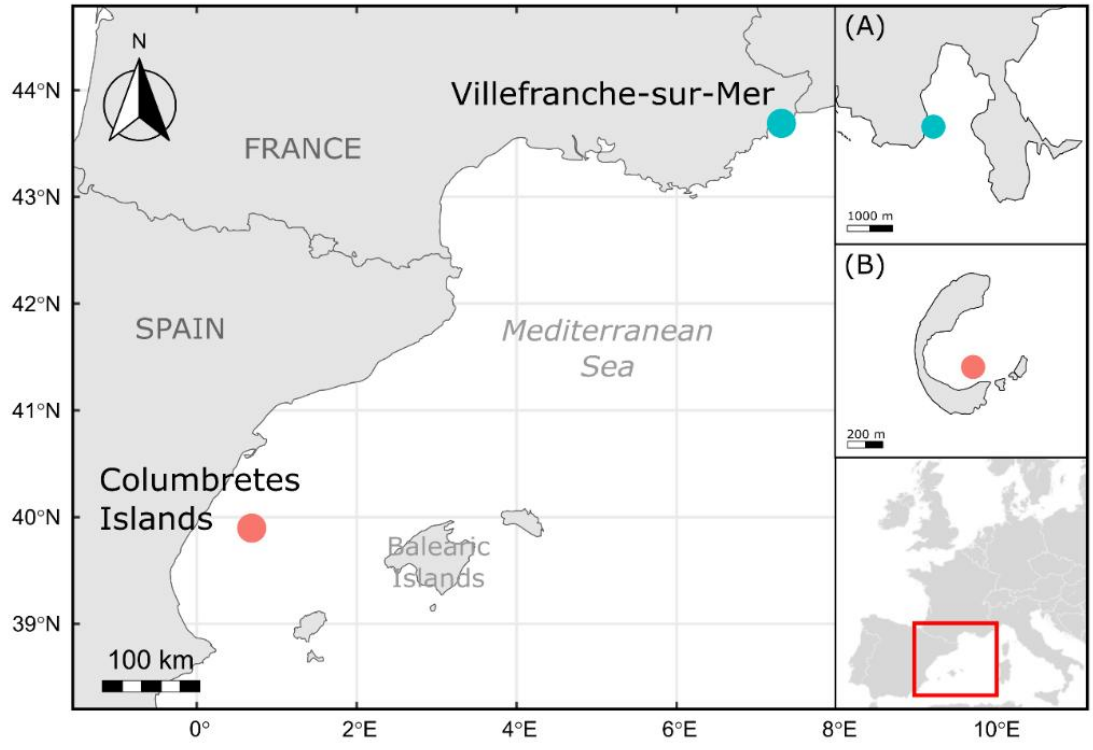

Figure 1. Location of study sites in the NW Mediterranean: Villefranche-sur-Mer (blue, A), and Columbretes Islands (red, B).

2.2 Environmental data

In the Columbretes Islands, *in situ* temperature and pH data have been collected in the bay of Illa Grossa at the same location and depth (15 m) as the coral population. Temperature has been recorded daily since 2007, using an autonomous HOBO v2 Water Temp Pro sensor (Kersting et al., 2025), while pH_{sw} was recorded between October 2024 and August 2025 using a pH-Log3030 glass electrode sensor. The sensor recorded pH hourly, in NBS scale, which was converted to pH_{SWS}, and finally pH_T (hereafter referred to as *in situ* pH_{sw}), using respectively the "pHnbs2sws" and "pHconv" functions of the "seacarb" v3.3.3 R package (Gattuso et al., 2015b), and setting salinity at 38.14 UPS. For consistency with the Villefranche data, only the data from 9:00 local time (LT) were used. In Villefranche, *in situ* temperature data at 10 and 15 m have been collected since 1992 from weekly CTD casts made between 0 and 80 m depth (Mousseau et al., 2024). The average *in situ* temperature was calculated from the data measured at 10 and 15 m depth. Seawater carbonate chemistry parameters (total alkalinity, A_T, DIC) have been recorded weekly in Point B, since 2007, at 1 and 50 m depth, at 9:00 LT, and used to calculate pH_T (hereafter referred to as *in situ* pH_{sw}) (Gattuso et al., 2021). Here, only the data from 1 m depth were used. Weekly averages were obtained

https://doi.org/10.5194/egusphere-2026-2720
Preprint. Discussion started: 29 May 2026

for all environmental data products. The 24h pH_{sw} measurements for the Columbretes Islands are shown in comparison to pH_{sw} for Villefranche in Fig. B2.

2.3 Geochemical analysis

Cleaned individual corallites were fixed to a Plexiglas base and cut longitudinally with a microtomic water-cooled saw. One half of each corallite was selected for geochemical analyses and further cleaned in an ultrasonic bath with ultra-pure (18.2 MΩ) water for 15 min and dried at room temperature for 24h.

2.3.1 Femtosecond laser ablation MC-ICP-MS and correction of scattered Ca ion interference

In situ boron isotopes were determined for each corallite at the Helmholtz Laboratory for Geochemistry of Earth Surface (HELGES) at the GFZ Helmholtz Centre for Geosciences, Potsdam, using a custom-built UV femtosecond laser ablation system (fsLA, details about the setup and performance can be found in Schuessler and von Blanckenburg 2014). The fsLA is coupled with a *Thermo Neptune* multi-collector inductively coupled plasma mass spectrometer (MC-ICP-MS) equipped with a Jet interface. Prior to analysis, the fsLA-MC-ICP-MS was tuned for maximum sensitivity, ensuring the adequate analysis of boron isotopes. The corallites were analysed along the growth axis in rectangular raster patterns starting from the calix. Each section consisted of rectangular laser paths ~50 µm wide by 600 µm long (± 50 µm depending on the average linear extension rate of each corallite sample, Table B1). This sampling strategy resulted in an approximate monthly to bimonthly sampling resolution. The laser paths were set exclusively on the internal part of the skeletal wall, avoiding other skeletal structures or the external part of the wall to reduce the risk of diagenetic contamination (Montagna et al., 2007). Each path was ablated and measured twice using a laser spot size of ~20 µm diameter, with an ablation frequency of 166.7 Hz and a scan speed of 38 $\mu m \cdot s^{-1}$. The typical operating conditions of the laser are reported in the Table B2. ^{11}B and ^{10}B signals were collected in cups H4 and L4, both equipped with 10^{13} Ω resistors. Data was collected over 500 cycles of 0.547 s, with samples ablated in the first ~250 cycles, washing out over the following ~200 cycles, and gas blank signals analysed in the last ~50 cycles. Data evaluation was done manually offline and involved subtraction of the average ^{11}B and ^{10}B background signal intensity (on-peak gas blank integrated over ~50 cycles after each ablation) from each cycle before boron isotope ratio was computed.

To monitor and correct for scattered Ca ions ($Ca_{interference}$; see Sadekov et al., 2019; Standish et al., 2019), signal at m/z 10.066 was also monitored with a 10^{13} Ω resistor on L3. Matrix interferences were then corrected by fitting a power relationship between the $\delta^{11}B$ inaccuracy and the non-blank corrected $^{11}B/Ca_{interference}$ (Fig. B3) determined from a set of certified and in-house reference carbonates, via a method modified from Standish et al. (2019) and Evans et al. (2021). Standards included two calcite crystals (DE-B and DE-Y, Table B3, Coenen et al., 2024a, b), pressed powder MACS-3 supplied by USGS (Jochum et al., 2012), three pellets pressed at HELGES of reference carbonates JCp-1 and JCt-1 (Inoue et al., 2004; Okai et al., 2002) and

https://doi.org/10.5194/egusphere-2026-2720
Preprint. Discussion started: 29 May 2026

in-house brachiopod carbonate MVS-1 (Jurikova et al., 2020). To ensure comparability with solution MC-ICP-MS measurements, JCp-1, DE-B and DE-Y were also measured via solution at HELGES (see Table B3), using methods detailed in Section 2.2.3 below and in Ring et al. (2025). Within an analytical session on fsLA-MC-ICP-MS, typically two blocks of reference materials would bracket every 10 coral sub-samples, with each block of reference materials bracketed by two NIST SRM610 glass standards (Standish et al., 2019). Each standard was ablated at a speed of 38 µm·s^{-1} and a frequency of 500 Hz, except for NIST SRM610 which was ablated at a frequency of 166.7 Hz, to keep ^{11}B signal below the ~500 mV maximum capacity for the 10^{13} Ω resistors. To monitor performance and reproducibility within each run, *Porites* spp. coral reference material JCp-1-NP (Jochum et al., 2019; Okai et al., 2002) was measured (Table B4), although we note that likely due to contamination from non-carbonate phases during the nano-milling procedure, absolute δ^{11}B values were found to be isotopically lighter than powdered JCp-1. While we analysed a sample of the nano-pellet material via solution MC-ICP-MS (obtaining a δ^{11}B value of 21.99 ‰), our cleaning and dissolution protocol was not designed for non-carbonate matrices, and thus may not have incorporated lighter agate-phase B that would be entrained in a laser analysis. As such, comparison with solution measurements is difficult.

2.3.2 Trace elements

Elemental compositions of Li, B, Mg, Sr and Ca, were determined by setting ablation paths directly next to the isotopic measurement paths. Samples C3-1, C3-2, C3-3, V3-2, and V3-3 were analysed using the same fsLA used for isotopic analysis, coupled with a *Thermo* iCAP quadrupole ICP MS (fsLA-iCAP-Qc-ICP-MS) at HELGES. Samples V3-1 and C3-7 were analysed using a nanosecond laser at the EleMap lab (GFZ Helmholtz Centre for Geosciences, Potsdam, Vergotti et al., 2025a), and GEOMAR (Helmholtz Centre for Ocean Research, Kiel) facilities, respectively. Both samples were measured in continuous transects covering the whole length of the corallite by ablating the wall section of the skeletons, after performing a pre-ablation scan. For comparability with the sampling method of the boron isotope data, the trace element values obtained from the ns lasers were separated in longitudinal sections of 600 ± 50 µm along the laser transect. All trace element data were reduced using the *Iolite v4* software (https://iolite.xyz/, Paton et al., 2011; Woodhead et al., 2007), setting the glass standards NIST SRM610 and NIST SRM612 as external reference standards and element ^{43}Ca as internal element standard (Jochum et al., 2011). The LA-ICP-MS settings and the typical operating conditions are specified in Table B2. Performance and reproducibility were monitored measuring JCp-1-NP (Hathorne et al., 2013; Jochum et al., 2019; Okai et al., 2002), and the resulting mean line values and standard deviations are given in Table B5.

2.3.3 Chemical separation of boron isotopes

To cross-validate boron isotopic measurements performed by laser ablation, additional boron isotopic measurements were performed on one corallite sample of the Columbretes Islands (sample C3-2) using solution MC-ICP-MS at HELGES. The

https://doi.org/10.5194/egusphere-2026-2720
Preprint. Discussion started: 29 May 2026

pre-cleaned second half of sample C3-2 was emptied of all septa using a hand-saw, leaving only the outer skeletal wall. The emptied corallite was then cleaned in an ultrasonic bath with ultra-pure water for 15 minutes and dried at room temperature for 24h. Powder subsamples were collected with a computer-controlled micro-mill along the growth axis in increments of 55 µm to match the sampling resolution used for laser ablation. The skeleton still occupied by living tissue at the time of collection (~0.35 cm, Peirano et al., 2005) was excluded to minimize risks of organic contamination. The powder subsamples, each weighing ~25 µg were oxidatively cleaned prior to dissolution in double distilled 0.5M HNO_3 following methods outlined by Stewart et al. (2016). Boron was separated from the carbonate matrix using anion exchange chromatography columns and measured against NIST SRM 951 with a *Thermo Neptune* MC-ICP-MS following Ring et al. (2025). Boron blanks from column procedures were measured, and samples corrected for blank contribution via mass balance. External reproducibility was estimated by repeat measurements of carbonate standard JCp-1 (Okai et al., 2002). Intermediate reproducibility and machine behaviour were monitored with boric acid standard ERM-AE121 (Vogl and Rosner, 2012) measured at different concentrations (see Table B3 for values).

2.4 Data analysis

The age models of the $\delta^{11}B$ coral records were established based on the relationship of two sets of element ratios with the weekly *in situ* temperature data, using the date of collection of the samples to fix the chronology. The elemental ratios records used to establish the age models included: Sr/Ca, B/Ca, Li/Mg and B/Mg ratios, using the specific combination that presented the best seasonal signal for each corallite, with the best match with the seasonality of temperature. To compare elemental ratios obtained from different instruments, a normalization was applied to eliminate potential instrumental bias, as JCp-1-NP presented different elemental ratios between instruments. Accordingly, for each site separately, the elemental ratios were normalized by subtracting the average corresponding to each corallite and adding the overall average elemental ratio of all corallites.

Detailed calculations for pH and other parameters of the carbonate system are provided in Appendix A. Briefly, pH_{cf} was calculated from $\delta^{11}B$ following the methodology described by Trotter et al. (2011), and the carbonate chemistry parameters (CO_3^{2-}, $B(OH)_4^-$, DIC_{cf}, and Ω_{cf}) from $\delta^{11}B$ and B/Ca, following the methodologies outlined in D'Olivo and McCulloch, 2017, Holcomb et al., 2016, and McCulloch et al., 2017. The magnitude of pH upregulation (ΔpH) was calculated as the difference between pH_{cf} and *in situ* pH_{sw}. For consistency with the Columbretes Islands (with pH_{sw} measurements covering only the period from October 2024 to August 2025), ΔpH for Villefranche was calculated using the *in situ* pH_{sw} averaged by month.

https://doi.org/10.5194/egusphere-2026-2720
Preprint. Discussion started: 29 May 2026

2.4.1 Statistical tests

The interference correction method was validated with a one-way ANOVA, comparing the $\delta^{11}B$ records for sample C3-2 obtained from laser ablation and from solution analysis. The reconstructed monthly coral pH_{sw} records from Villefranche were compared in the same way with the monthly *in situ* pH_{sw} records. Differences between sites were tested with one-way ANOVA, using monthly geochemical data from each sample ($\delta^{11}B$, B/Ca, DIC_{cf}, Ω_{cf}, and pH_{cf}), and the corresponding seasonal (warm and cold season) growth data (linear extension, skeletal density, and calcification). Q-Q plot inspection showed no substantial deviation from the assumptions of normality and homoscedasticity. Differences of *in situ* temperature between sites over the period covered by the corals (June 2016 to February 2022) were evaluated applying a linear mixed-effects model to weekly averaged data, using the "lmer" function of the *lme4* R package (Bates et al., 2014), with sites as a fixed effect and week as a random effect to account for seasonal autocorrelation. The reconstructed pH_{sw} of both sites was assessed for long-term trend using a generalized least-squares (GLS) model using the "gls" function of the *nlme* R package (Pinheiro et al., 2020). To account for temporal autocorrelation, the reconstructed pH_{sw} was set as the response variable, time as the fixed effect, and samples as a grouping factor to incorporate a first-order autoregressive (AR1) correlation structure. The effect of environmental parameters (*in situ* temperature, pH_{sw}, DIC_{sw}, and Ω_{sw}) on the reconstructed pH_{cf} and DIC_{cf} of the Villefranche corals was tested by fitting a multi-linear model setting the monthly average reconstructed parameter as the response variable, and the average monthly environmental parameters for the period covered by the corals (December 2015 to February 2022) as the explanatory variables. The variables for the best-fit model were selected using the stepwise backward-forward method, starting from the model containing all possible explanatory variables (full-model), and using the Bayesian Information Criterion (BIC). The stepwise model selection used the "stepAIC" function of the *MASS* R package (Venables and Ripley, 2002). The ΔBIC was then calculated as the difference between the BICs of the full model and the model without the target variable as a measure of variable importance. The assumptions of the model were evaluated using the "check_model" function of the *performance* R package (Lüdecke et al., 2021), showing no substantial deviation from the assumptions of normality and homoscedasticity. The collinearity of the variables was evaluated with the variance inflation factor (VIF), using the "vif" function of the *car* R package (Fox and Weisberg, 2018). As the VIF test revealed a high level of multicollinearity among the explanatory variables (VIF > 10), a principal component regression (PCR) was used to calculate the correlation coefficients of environmental variables with pH_{cf} and DIC_{cf}, using the "pcr" function of the *pls* R package (Liland et al., 2024), using centred and scaled explanatory variables and a 10-fold cross-validation to determine the optimal number of components. The annual seasonality of the *in situ* carbonate chemistry parameters, *in situ* temperature of Villefranche, and coral carbonate chemistry records of each site were reconstructed by averaging all available data for each month. The data of each site were then centred by subtracting the overall mean value of each record from its monthly values, so that all records have a mean of zero while conserving their respective standard deviation.

https://doi.org/10.5194/egusphere-2026-2720
Preprint. Discussion started: 29 May 2026

3 Results

3.1 Regional scale variability in *in situ* pH_{sw} and temperature

Average pH_{sw} in Villefranche was 8.07 ± 0.05 for the 2015 to 2023 period. In the Columbretes Islands, the average pH_{sw} was 8.15 ± 0.07 at 9:00 LT, and the daily mean 8.15 ± 0.06 (using 24 daily measurements), between October 2024 and August 2025. Seasonal pH_{sw} minima in Villefranche, of 7.98 on average, occurred between July and August, and maxima of 8.12 on average between February and March. In the Columbretes, at 9:00 LT, minima of 8.08 on average occurred in June, and maxima of 8.31 on average occurred in February (Fig. 2). It should be noted that the entire year was not measured in the Columbretes Islands, making it difficult to estimate the seasonal low with certainty.

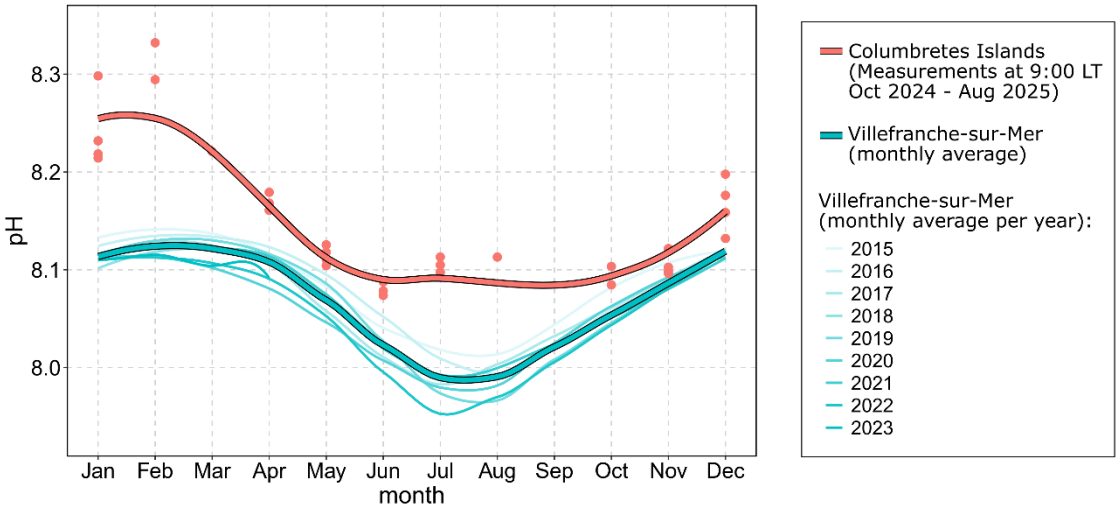

Figure 2. Average monthly pH_{sw} measured at 9:00 LT, at 15 m in the Columbretes Islands between October 2024 and August 2025 (bold red), and measured at 1 m in Villefranche between 2007 and 2023 (bold blue), represented using a loess smoothing factor for visualization purposes. For the Columbretes Islands, average weekly values are shown (red dots). Monthly profiles for individual years for Villefranche are also included (thin lines).

The *in situ* temperature record of the Columbretes Islands between 2015 and 2022, with an average annual temperature of 19.06 ± 4.45 °C, was significantly warmer by an average of 0.48 ± 0.06 °C than in Villefranche, with an average annual temperature 18.38 ± 3.86 °C (t = -8.28, n = 1026), mostly due to colder summers in Villefranche. Summer temperatures were of 24.78 ± 1.67 on average for the Columbretes Islands, and of 23.47 ± 1.64 for Villefranche.

https://doi.org/10.5194/egusphere-2026-2720
Preprint. Discussion started: 29 May 2026

3.2 Geochemical composition of the coral CF

Significantly higher linear extension rates and calcification rates were found in the Columbretes Islands (4.07 ± 0.88 mm·yr^{-1} and 0.27 ± 0.07 g·cm^{-2}) compared to Villefranche (3.09 ± 0.96 mm·yr^{-1} and 0.20 ± 0.07 g·cm^{-2}) (Table 1, Table B1, Table B7). Additionally, significantly lower B/Ca, Ω_{cf}, pH_{cf} and reconstructed pH_{sw}, and higher DIC_{cf} were found in the Columbretes Islands, compared to Villefranche (Fig. 3, Table 1, Table B6, Table B7). Overall, the values of B/Ca measured in this study were within the range of variation reported by Montagna et al. (2007) for the same species (600 to 1000 µmol·mol^{-1} compared to 600 to 900 µmol·mol^{-1} in the present study).

Table 1. Summary of the comparison of environmental and biological parameters between Villefranche-sur-Mer and the Columbretes Islands. Arrows indicate the site with the highest or lowest parameters. Average values ± SD are shown in parenthesis. Significant differences the biological parameters of each site were evaluated with ANOVA, which are summarized in Table B7.

	Villefranche-sur-Mer	Columbretes Islands
Environmental parameters		
Location	North	South
Coastal influence	↑	↓
In situ temperature	↓ (18.38 ± 3.86 °C)	↑ (19.06 ± 4.45 °C)
Average *in situ* summer temperature	↓ (23.47 ± 1.64 °C)	↑ (24.78 ± 1.67 °C)
pH (at 9:00 LT)	↓ (8.07 ± 0.05 pH units) * **(between 2007 and 2022)*	↑ (8.15 ± 0.07 pH units) * **(between 2024 and 2025)*
Biological parameters		
Linear extension	↓ (3.09 ± 0.96 mm·yr^{-1})	↑ (4.07 ± 0.88 mm·yr^{-1})
Skeletal density	= (1.35 ± 0.20 g·cm^{-3})	= (1.31 ± 0.20 g·cm^{-3})
Calcification	↓ (0.20 ± 0.07 g·cm^{-2})	↑ (0.27 ± 0.07 g·cm^{-2})
$\delta^{11}B$	↑ (25.71 ± 0.97 ‰)	↓ (24.55 ± 1.06 ‰)
B/Ca	↑ (782 ± 62 µmol·mol^{-1})	↓ (694 ± 62 µmol·mol^{-1})
DIC_{cf}	↓ (2890 ± 222 µmol·kg^{-1})	↑ (3363 ± 319 µmol·kg^{-1})
Ω_{cf}	↑ (13.28 ± 1.24)	↓ (13.77 ± 1.55)
pH_{cf}	↑ (8.67 ± 0.09 pH units)	↓ (8.58 ± 0.09 pH units)

The corals of Villefranche had an average $\delta^{11}B$ composition of 25.68 ± 0.94 ‰ ranging from 25.34 ± 0.84 ‰ to 26.04 ± 0.98 ‰ (Table B6), which is very similar to the range of 25.1 to 26.7 ‰ reported by Trotter et al. (2011) for *C. caespitosa* across a range of ambient pH (8.07 to 8.1, Fig. 3). The corals from the Columbretes Islands had a significantly lower average $\delta^{11}B$ of

https://doi.org/10.5194/egusphere-2026-2720
Preprint. Discussion started: 29 May 2026

24.55 ± 1.06 ‰ (Table 1, Table B7), ranging from 24.15 ± 0.85 ‰ to 25.05 ± 0.96 ‰, putting them on the lower range of variability reported by Trotter et al. (2011).

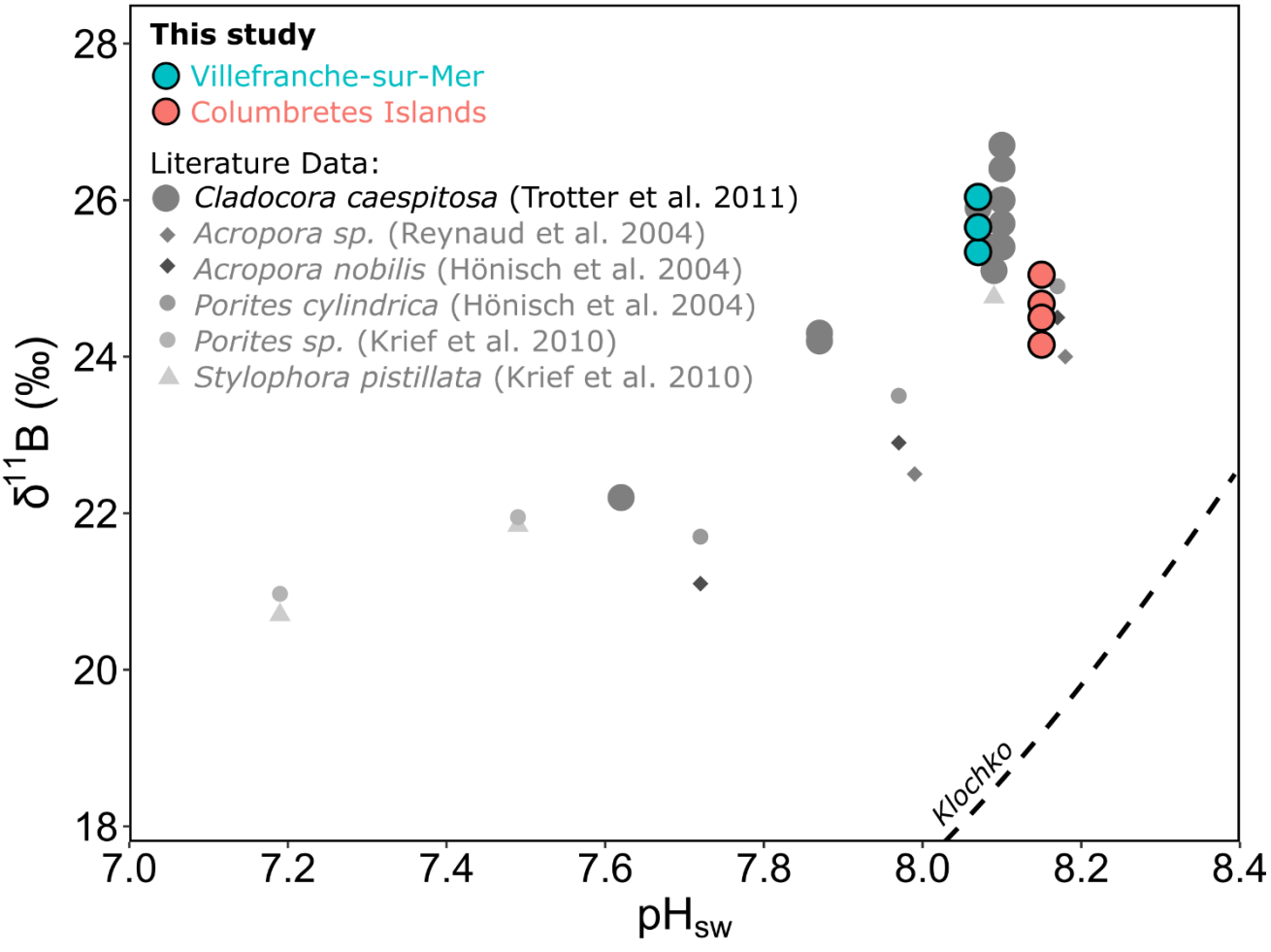

Figure 3. Average coral $\delta^{11}B$ for individual corallites from Villefranche (blue) and the Columbretes Islands (red) relative to average *in situ* pH_{sw}. In Villefranche, the average *in situ* pH_{sw} was of 8.07 between 2015 and 2022, while the average *in situ* pH_{sw} for the Columbretes Islands was of 8.05 between October 2024 and August. The reference borate curves (Klochko et al., 2006) are also shown in dashed lines. Measurements from shallow water tropical corals obtained from the literature, as well as for *C. caespitosa* in a previous study by Trotter et al. (2011) are shown in grey scales.

3.2.1 $\delta^{11}B$ measured via LA and solution chemistry

No significant difference in absolute $\delta^{11}B$ values was found between measurements obtained using LA and solution chemistry for sample C3-2 ($F_{1,44}$ = 0.09, p = 0.767), with both methods yielding mean compositions of 24.22 ± 1.00 ‰ and 24.15 ± 0.45

https://doi.org/10.5194/egusphere-2026-2720
Preprint. Discussion started: 29 May 2026

‰, respectively. Noticeably, the records obtained with chemical separation had a much lower seasonal range (± 1.67 ‰) compared to the records obtained with LA (± 4.63 ‰) (Fig. 4).

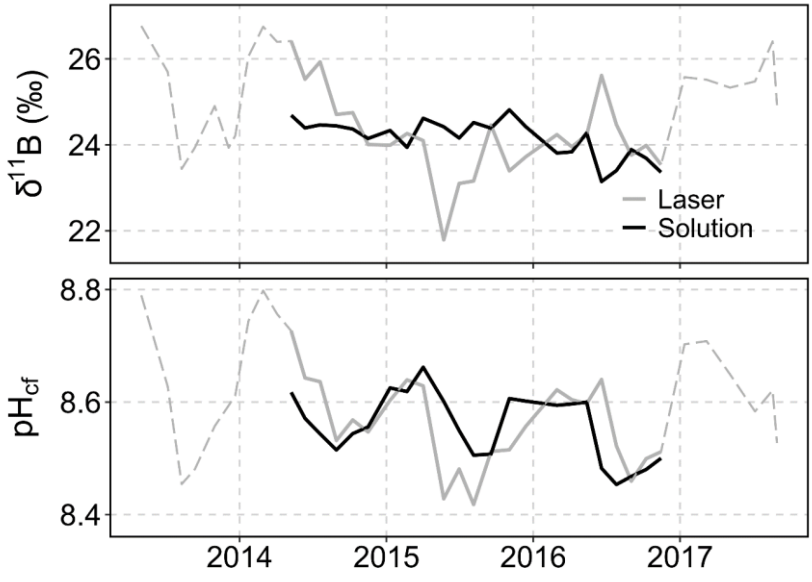

Figure 4. Time series of $\delta^{11}B$ and reconstructed pH_{cf} for the sample C3-2 from the Columbretes Islands, using LA (grey) and solution chemistry (black). The dashed line represents the full record measured with laser ablation for this sample.

3.3 Annual and seasonal variability of the CF composition

Average monthly B/Ca composition of both sites (Fig. 5c) presented oscillations consistent with seasonal variability as established based on skeletal annual density banding. Six cycles were identified in the corals of Villefranche, covering a period ranging from December 2015 to February 2022, while five cycles were identified in the corals of the Columbretes Islands, covering a period ranging from June 2013 to August 2017 (Fig. 5).

https://doi.org/10.5194/egusphere-2026-2720
Preprint. Discussion started: 29 May 2026

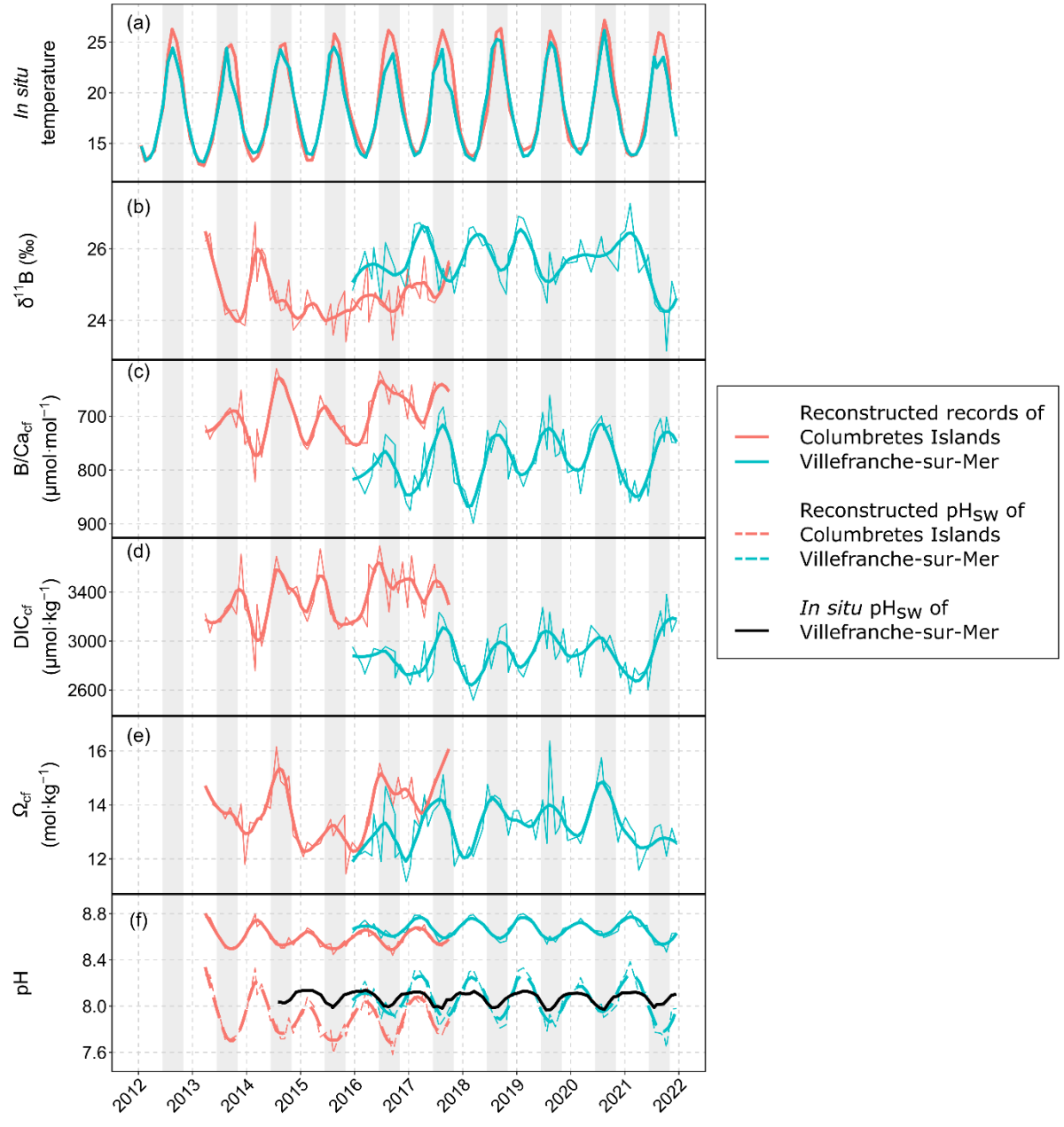

Figure 5. Time series of monthly temperature (a), coral $\delta^{11}B$ (b) and B/Ca (b) composition, and reconstructed carbonate records of DIC_{cf} (d), Ω_{cf} (e), and pH (f), where pH_{cf} is in full lines and reconstructed pH_{sw} in dashed lines. The records are represented for Villefranche (in blue) and the Columbretes Islands (light red). Environmental records of *in situ* pH_{sw} for Villefranche are also included (f, black). Grey vertical boxes highlight warm periods. A z-score test was run to identify and remove outliers (z-score > 3), resulting in the removal of 1 point. Coral records in panels b to f are presented as monthly data (thin lines) and after applying a loess smoothing factor of 1.9 (bold lines).

https://doi.org/10.5194/egusphere-2026-2720
Preprint. Discussion started: 29 May 2026

Overall, the seasonality of DIC_{cf}, Ω_{cf}, and particularly $\delta^{11}B$ in both sites was not as regular as for B/Ca or the reconstructed pH records (Fig. 5b, d, e), with muted seasonal cycles of $\delta^{11}B$, and particularly DIC_{cf} and Ω_{cf}, occurring in the records of the Columbretes Islands, during the summer 2015. The oscillation of the $\delta^{11}B$ derived pH records (pH_{cf} and pH_{sw}, Fig. 5f) were in phase with the B/Ca data and inversely related to *in situ* temperature. The average seasonal amplitude of the reconstructed pH_{cf} in Villefranche and in the Columbretes Islands was of 0.2 pH units, with maxima occurring in February and March, and minima occurring in August and September respectively (Fig. 6d). The average coral-reconstructed pH_{sw} of 8.06 ± 0.19 for Villefranche was not significantly different from the *in situ* pH_{sw} data ($F_{1,139} = 0.280$, $p = 0.598$), and both series were positively correlated ($r^2 = 0.473$, $p < 0.001$). The timing of the seasonal oscillation of the reconstructed pH_{cf} and instrumental pH_{sw} of Villefranche mostly agreed (Fig. 5f), with winter maxima occurring in February, coinciding with the winter low in temperature (Fig. 6a and d). Nevertheless, both reconstructed pH_{cf} and *in situ* pH_{sw} presented a lag of approximately one month in their summer extremes (Fig. 6d). The pH_{cf} minimum occurred in August, coinciding with the summer maximum of *in situ* temperature, while the minimum of pH_{sw} occurred in July. The seasonal oscillation of pH_{cf} in the Columbretes Islands coincided more closely with the inverse seasonal oscillation of temperature, rather than *in situ* pH_{sw}. The seasonal amplitude of reconstructed pH_{sw} in Villefranche (on average, 8.26 in winter and 7.89 in summer) more than doubled the *in situ* pH_{sw} (on average, 8.12 in winter and 7.98 in summer). Average annual seasonality of the reconstructed DIC_{cf} of corals from both sites was inversely related with *in situ* DIC_{sw} (Fig. 6b). In the case of the Villefranche corals, the seasonality of DIC_{cf} closely matched that of *in situ* temperature, while the seasonal pattern was less clear in the case of the Columbretes Islands, with a maximum in June followed by a soft decline until the minimum in February (Fig. 6a and b). For both sites, the seasonal variability of Ω_{cf} was very low, with only a marked maximum between July and August, fitting closely with the summer maxima of *in situ* temperature (Fig. 6c). However, both the reconstructed DIC_{cf} and Ω_{cf} of the Villefranche corals presented a higher range of variation than the measured *in situ* DIC_{sw} and Ω_{sw} (Fig. 6b and c), with the average DIC_{cf} and Ω_{cf} being respectively x1.3 and x4.1 time greater than the average DIC_{sw} (2260 ± 21 $\mu mol \cdot kg^{-1}$) and Ω_{sw} (3.25 ± 0.23 units). The ΔpH of Villefranche (0.60 ± 0.07), was on average higher than the inferred ΔpH of the Columbretes Islands (0.45 ± 0.08). ΔpH in Villefranche was not constant through the year, with highest values in March, and lowest in October (Fig. 6e). In turn, ΔpH in the Columbretes Islands reached its highest values in April, while the lowest values occurred in February (Fig. 6e), although this record reflects a single incomplete year of *in situ* pH_{sw} measurements.

https://doi.org/10.5194/egusphere-2026-2720
Preprint. Discussion started: 29 May 2026

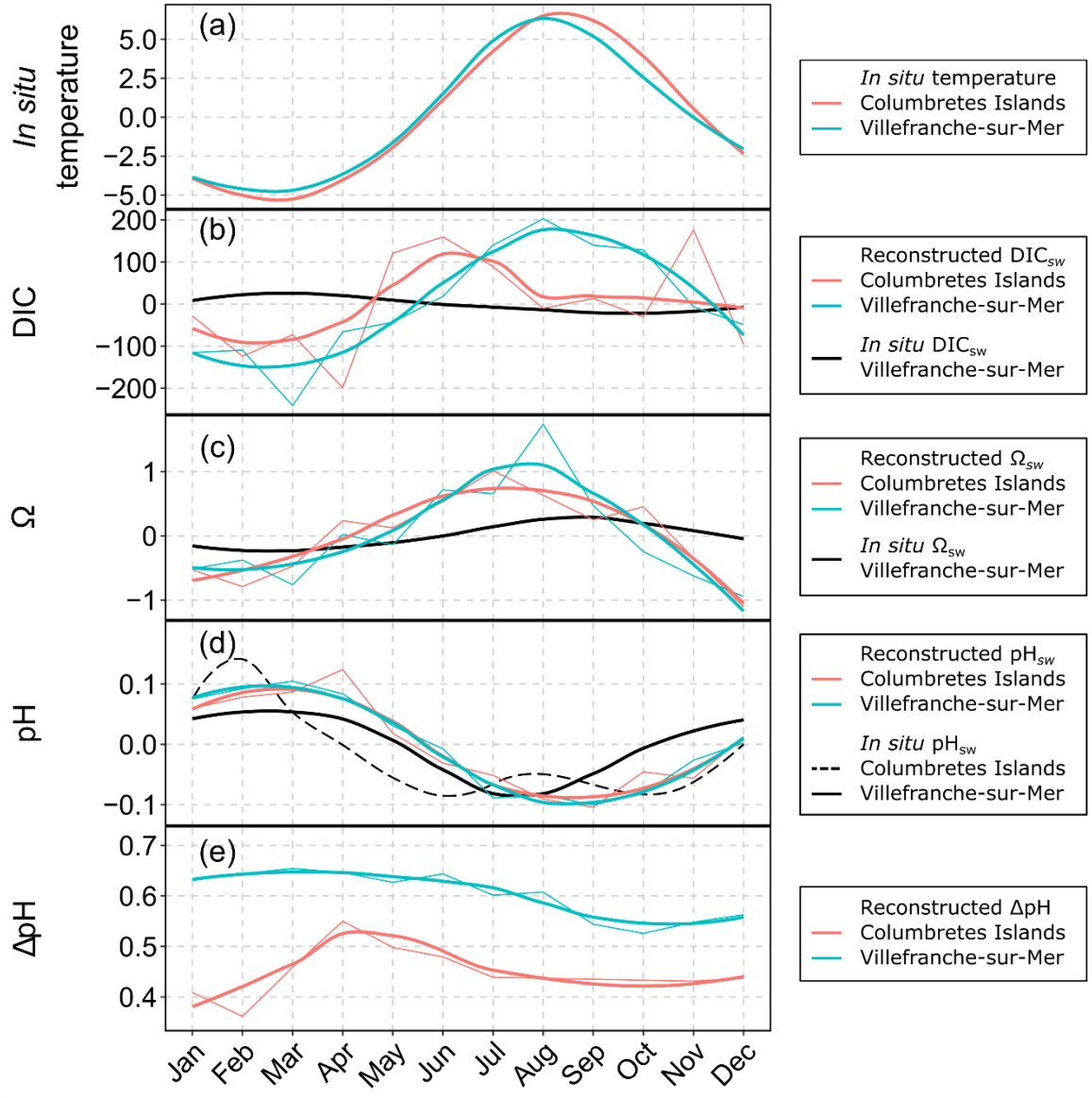

Figure 6. Average monthly plots of seawater temperature and carbonate chemistry in Villefranche (blue) and the Columbretes Islands (red): (a) *in situ* temperature (b) reconstructed DIC_{cf} for both sites and *in situ* DIC_{sw} of Villefranche (black), (c) reconstructed Ω_{cf} for both sites with *in situ* Ω_{sw} of Villefranche (black), (d) reconstructed pH_{cf} for both site with *in situ* pH_{sw} of Villefranche (black, solid) and Columbretes Islands (black, discontinuous), and (e) ΔpH of both sites. The records of *in situ* temperature, DIC, Ω, and pH are presented as centred on a mean of 0. All records are presented as average monthly data (thin lines) and after applying a loess smoothing factor (bold lines). The average used data from 2013 to 2017 for the Columbretes Islands, and from 2015 to 2022 for Villefranche.

No significant long-term trend was observed in the reconstructed pH_{sw} of either the Columbretes Islands (t = -1.19, p = 0.24), or Villefranche (t = -0.80, p = 0.42).

https://doi.org/10.5194/egusphere-2026-2720
Preprint. Discussion started: 29 May 2026

3.3.1 Environmental factors acting on the composition of the CF

For pH_{cf}, the stepwise AIC test identified temperature as the primary environmental predictor, followed by pH_{sw}. PCR further indicated both variables were positively correlated to pH_{cf} (Table 2). In the case of DIC_{cf}, only temperature was identified by the stepwise AIC test as the most relevant environmental variable, with a positive effect (Table 2).

Table 2. Multivariate analysis correlating the reconstructed pH_{cf} and DIC_{cf}, with *in situ* temperature and pH_{sw} of the seawater. The standardized regression coefficients (β^{S}_{PC}) obtained with the principal components regression (PCR) are presented for the full model, and the ΔBIC for the most relevant variables identified with the stepwise AIC test are indicated. The variance explained by the two components of the PCR is indicated by the coefficient of determination (r^2).

	β^{S}_{PC}	ΔBIC	VIF	r^2
Effects on pH_{cf}				
Temperature	-0.023	-18.56	24.33	
pH_{sw}	0.025	-5.46	12.37	
DIC_{sw}	0.010	Excluded	2.85	
Ω_{sw}	-0.016	Excluded	7.02	
Model				0.679
Effects on DIC_{cf}				
Temperature	32.09	3.39	24.33	
pH_{sw}	-27.78	Excluded	12.37	
DIC_{sw}	-30.04	Excluded	2.85	
Ω_{sw}	32.45	Excluded	7.02	
Model				0.323

4 Discussion

4.1 Reconstructing pH_{sw} in temperate corals

The $\delta^{11}B$ records obtained with fsLA (laser ablation) were broadly consistent with those obtained through solution MC-ICP-MS, indicating a reliable measurement of the $\delta^{11}B$ and an adequate correction of the interference occurring with the fsLA. However, the lower variability of the records obtained through chemical separation hint at the challenge of sampling specific

https://doi.org/10.5194/egusphere-2026-2720
Preprint. Discussion started: 29 May 2026

skeletal structures when using bulk sampling methods, with part of the $\delta^{11}B$ records being possibly altered by remnants of other skeletal structures of the corallites (Chalk et al., 2021). Additionally, owing to the often-complex 3D structure of *C. caespitosa* corallites, the powder sampling process is not always perpendicular to the growth axis, mixing skeleton material of different time periods, and leading to an unintended smoothing of the records. These issues underline the advantage of using *in situ* methods such as fsLA for long-term high-resolution environmental reconstructions, as it allows a high level of precision and selectivity in the sampling of skeletal structures (Chalk et al., 2021; Evans et al., 2021).

Further highlighting the potential of using fsLA, the agreement of the reconstructed and *in situ* pH_{sw} of Villefranche indicates a good applicability of the equation proposed by Trotter et al. (2011) for *C. caespitosa* from this population. Nevertheless, the pH_{sw} reconstructed from the Villefranche corals presented a higher range of variability than *in situ* pH_{sw}. In tropical corals, seasonal amplification of pH upregulation is believed to offset the large seasonal swings in DIC_{cf} caused by environmentally driven symbiont activity (D'Olivo and McCulloch, 2017; McCulloch et al., 2017; Ross et al., 2017). Further, the pH_{sw} reconstructed in the Columbretes Islands (7.88 ± 0.20 on average) was significantly lower than Villefranche, and below the pH_{sw} of 8.15 ± 0.07 measured *in situ* in the Columbretes Islands between October 2024 and August 2025. The Columbretes Islands are further south and less coastal than Villefranche and ambient pH sites sampled by Trotter et al. (2011). These environmental differences likely impose a distinct set of controls on the CF composition of the Columbretes Islands corals. Indeed, this population had higher levels of DIC_{cf}, and also grew at higher temperatures, particularly during the summer. Since DIC_{cf} is thought to be primarily supplied by coral-symbiont metabolism (Comeau et al., 2017a; Furla et al., 2000; Pearse, 1970), higher temperatures during the summer in Columbretes Islands may enhance coral metabolic activity and respiration rates relative to symbiont metabolic rates, thus increasing DIC_{cf} (Guo, 2019; Kersting et al., 2025; Ross et al., 2017, 2019), also contributing to decrease pH_{cf}.

Additional differences in light and nutrient availability, for example due to differences in terrestrial influence, may alter the metabolic activity of the symbionts, further differentiating the CF composition between sites (Dissard et al., 2012; Ross et al., 2022; Thil et al., 2016). Confirming the causes for these inter-population differences would require expanded monitoring of *in situ* pH_{sw}, light and nutrients. These differences also highlight limitations for the $\delta^{11}B$-pH calibration curve for *C. caespitosa* proposed by Trotter et al. (2011). Because it does not encompass the full range of environmental variability across populations, applying this calibration may result in reconstructed pH_{sw} values that deviate from true *in situ* conditions, highlighting the need to expand calibration datasets to include a wider diversity of environments, and to have specific calibrations for each environment (Guo, 2019).

4.2 Upregulation of pH_{cf} and DIC_{cf} in *Cladocora caespitosa*

The ΔpH levels observed in this study (0.60 ± 0.07 in Villefranche and 0.45 ± 0.08 in the Columbretes Islands) were comparable to previously reported values for *C. caespitosa* and appear higher than those of most tropical corals at ambient

https://doi.org/10.5194/egusphere-2026-2720
Preprint. Discussion started: 29 May 2026

pH_{sw} conditions (Comeau et al., 2017b; McCulloch et al., 2017; Trotter et al., 2011). Nevertheless, the slower growth dynamics of *C. caespitosa* – which result in lower carbonate requirements for calcification (Comeau et al., 2014, 2017b; Rodolfo-Metalpa et al., 2010; Trotter et al., 2011) – could facilitate maintaining a higher ΔpH compared to faster growing species. Further, *C. caespitosa* (this study) and tropical corals (D'Olivo et al., 2019a; McCulloch et al., 2017) displayed similar ranges of seasonal pH_{cf} variation despite pH_{sw} varying more strongly in Villefranche compared to tropical environments. This reduced variability suggests that *C. caespitosa* has a lower sensitivity to changes in pH_{sw}. However, both study sites presented relatively low DIC_{cf} with less seasonal variability compared to tropical corals (Comeau et al., 2017b; McCulloch et al., 2017). Thus, with pH_{cf} inversely related to DIC_{cf}, the reduced amplitude of DIC_{cf} seasonality likely contributed to lower the seasonal variability of pH_{cf}. While these outcomes hint at similar controls over the CF across coral species, decoupling the internal control of seasonal changes in DIC_{cf} from the external control of seasonal changes in pH_{sw} over the CF would require longer records, or targeted experimental studies.

As a result of the trade-off between upregulating pH_{cf} and DIC_{cf} (D'Olivo and McCulloch, 2017; McCulloch et al., 2017; Ross et al., 2017; Schoepf et al., 2017), Ω_{cf} maintained remarkably low seasonal and inter-annual variability, with values well above Ω_{sw}. With similar levels of Ω_{cf} across sites, these outcomes further highlight the capacity of *C. caespitosa* to control its CF composition despite seasonally and geographically variable environmental conditions (Carbonne et al., 2021; Hoogenboom et al., 2010; Rodolfo-Metalpa et al., 2010; Trotter et al., 2011). The timing of the seasonal maxima and minima, as well as the seasonal amplitude of Ω_{cf} in both sites was consistent with tropical corals (Canesi et al., 2024; D'Olivo and McCulloch, 2017; McCulloch et al., 2017), further underlining similar modes of CF regulation. Average Ω_{cf} values of 13.8 ± 1.5 in the Columbretes Islands, and 13.3 ± 1.2 in Villefranche place *C. caespitosa* on the lower end of the tropical corals (approximately 14 to 22; Canesi et al., 2023; McCulloch et al., 2017), which is consistent with the lower carbonate requirements and lower growth rates of this species.

Interestingly, the corals of the Columbretes Islands grew faster than those of Villefranche, despite similar Ω_{cf}, indicating that CF chemistry alone does not fully explain coral calcification rates. Indeed, the Columbretes Islands – which harbour one of the biggest *C. caespitosa* population of the Mediterranean Sea – may present an environmental setting driving a more efficient use of the products of calcification, resulting in an enhanced aragonite precipitation, without affecting the CF composition. Whether these calcification differences are driven solely by environmental forcing, or genetic differences between populations in biological regulation beyond CF chemistry deserves further investigation.

4.3 Environmental factors mediating the CF composition

The strong indirect effect of temperature exerted over DIC_{cf} and pH_{cf}, combined with the close inverse match between B/Ca and temperature seasonality implicates the latter as the main environmental controller of the CF composition, and thus of calcification (Knebel et al., 2021; Rodolfo-Metalpa et al., 2010; Ross et al., 2022). These outcomes align with prior research

https://doi.org/10.5194/egusphere-2026-2720
Preprint. Discussion started: 29 May 2026

on both temperate and tropical corals, showing that high temperatures had a greater effect on calcification rates than high pCO_2 on the short-term, and were often associated with declines in coral growth (Reynaud et al., 2003; Ries et al., 2010; Rodolfo-Metalpa et al., 2010). Accordingly, disruptions of the seasonality observed in the CF for summer 2015 coincided with a MHW which resulted in high mortality rates in Mediterranean benthic environments, particularly in the coral population of the Columbretes Islands (Darmaraki, 2019; Garrabou et al., 2022). Specifically, high values of B/Ca, along with disruptions in the seasonal pattern of DIC_{cf}, and low values of Ω_{cf} were observed in the corals of the Columbretes Islands, consistent with a thermal stress response that has been similarly reported in tropical species (D'Olivo et al., 2019b; D'Olivo and McCulloch, 2017; Schoepf et al., 2021). Such responses have been attributed to disruptions in the DIC upregulation, possibly resulting from an altered expression of the genes responsible for DIC transport to the CF (Bernardet et al., 2019; Schoepf et al., 2022). Nevertheless, no such disturbance was reflected in pH upregulation, underscoring the variable impact of thermal stress on the CF composition (Ross et al., 2022; Schoepf et al., 2021). Further, the lack of growth anomalies in the coral skeletons suggests that the sustained pH upregulation was sufficient to maintain Ω_{cf} above the minimum threshold needed for a normal coral calcification, highlighting the fundamental role of pH upregulation in maintaining a state of homeostasis necessary for coral calcification (D'Olivo and McCulloch, 2017).

While no trend was found in the reconstructed pH_{sw} of either site, the current OA trend of the Mediterranean Sea is estimated at 0.003 pH units·yr^{-1} (Hassoun et al., 2022; Kapsenberg et al., 2017; Yao et al., 2016). The absence of a trend in the reconstructed pH_{sw} records is likely related to their limited duration combined with the strong seasonal and interannual temperature-driven variations in pH_{cf} and DIC_{cf}, masking the long-term effects of OA. Nonetheless, the relationship between pH_{cf} and pH_{sw} indicates a sensitivity of *C. caespitosa* to changes of pH_{sw}, consistent with evidence that OA exerts a dominant control on coral carbonate chemistry over long-term scales (Comeau et al., 2019b; D'Olivo et al., 2019a). Supporting this, an *aquaria* experiment combining high pCO_2 with stress-like conditions (high temperatures and low nutritional input) resulted in decreasing calcification in *C. caespitosa* (Movilla et al., 2012). This negative sub-lethal response was attributed to an impaired pH upregulation due, not only to decreased pH_{sw}, but to the combined effect of high temperatures and low nutrient input not meeting the energetic requirements for pH upregulation. These results underline the deleterious combined effects of temperature, OA and nutrient-depletion on coral growth.

5 Conclusion

Cladocora caespitosa displays CF regulation mechanisms similar to most tropical corals. While it is unclear whether the low variability of pH_{cf} results only from a lower sensitivity to environmental variability, or from the interaction with other parameters of the CF carbonate system, the apparent high biological control of *C. caespitosa* over its CF denotes a potentially lower sensitivity to changes in pH_{sw}, at least on the short-term investigated in this study. The limited span of our coral records highlights the need for expanded records, also encompassing intercolonial variability, to fully understand the long-term impact

https://doi.org/10.5194/egusphere-2026-2720
Preprint. Discussion started: 29 May 2026

of OA. With temperature found to be the main control on seasonal changes in the CF of *C. caespitosa*, our records highlight the potentially heightened susceptibility of the biological controls on the CF to thermal stress – with other stressors such as OA and low nutrient availability potentially impairing coral CF regulation further. While future studies are needed to expand the geographical and temporal scope, out records are an important step in understanding how Mediterranean coral populations will respond to increasingly variable environmental conditions, particularly in the context of ongoing ocean warming and acidification.

6 Appendices

Appendix A pH and carbonate system parameters calculations

The internal pH of the calcifying fluid (pH_{cf}) was calculated from the measured $\delta^{11}B$ by applying the equation described by Zeebe and Wolf-Gladrow (2001):

$$pH_{cf} = pK_B - \log\left(\frac{\delta^{11}B_{sw} - \delta^{11}B_{carb}}{\alpha_{B3-B4} \cdot \delta^{11}B_{carb} - \delta^{11}B_{sw} + 1000 \cdot (\alpha_{B3-B4} - 1)}\right) \text{ (Eq. A1)}$$

Where $\delta^{11}B_{sw}$ represents the $\delta^{11}B$ in seawater ($\delta^{11}B_{sw}$ = 39.5, from Foster 2008) and $\delta^{11}B_{carb}$ represent the $\delta^{11}B$ in the coral samples, $\alpha_{B3\text{-}B4}$ represents the fractionation factor for isotope exchange between boric acid and borate ions in seawater, defined at 1.0272 by Klochko et al. (2006), and pK_B represents the dissociation constant of boric acid and was calculated according to Zeebe and Wolf-Gladrow (2001) using *in situ* salinity (S) and temperature (T, in kelvin):

$$-\log(pK_B) = exp\left(\frac{-8966.9 - 2890.53\sqrt{S} - 77.942 \cdot S + 1.728\sqrt{S^3} - 0.0996 \cdot S^2}{T} + 148.0248 + 137.1942\sqrt{S} + 1.62142 \cdot S - \left(24.4344 + 25.085\sqrt{S} + 0.2474 \cdot S\right) \cdot \ln(T) + 0.053105\sqrt{S} \cdot T\right) \text{ (Eq. A2)}$$

We used the $\delta^{11}B$-pH calibration curve described for *C. caespitosa* by Trotter et al. (2011) to infer seawater pH (pH_{sw}) from pH_{cf}:

$$pH_{sw} = \frac{1}{0.48} \cdot pH_{cf} - 10 \text{ (Eq. A3)}$$

The concentrations of borate ion and carbonate ion were calculated following D'Olivo and McCulloch (2017) and McCulloch et al. (2017), respectively, with K_B calculated from pK_B:

https://doi.org/10.5194/egusphere-2026-2720
Preprint. Discussion started: 29 May 2026

$$[B(OH)_4^-]_{cf} = \frac{[B_T]}{1+\frac{[H^+]}{K_B}} \cdot 1000\ in\ \mu mol \cdot kg^{-1}$$ (Eq. A4)

$$\left[CO_3^{2-}\right]_{cf} = K_{d,cf} \cdot \frac{[B(OH)_4^-]_{cf}}{[B/Ca]_{cf}} \cdot 1000\ in\ \mu mol \cdot kg^{-1}$$ (Eq. A5)

Where $[H^+]$ is calculated in mol·kg^{-1}, from pH_{cf}. The total boron concentration ($[B]_T$) was calculated following Zeebe and Wolf-Gladrow (2001), and the partition coefficient of B/Ca in aragonite ($K_{d,cf}$) is calculated following McCulloch et al. (2017), using $K_{d,0}$ = 0.00297 and K_{Kd} = - 0.0202:

$$[B_T] = 4.16 \cdot 10^{-4} \cdot \left(\frac{S}{35}\right) \cdot 1000\ in\ mmol \cdot kg^{-1}$$ (Eq. A6)

$$K_{d,cf} = K_{d,0} \cdot e^{-K_{Kd} \cdot [H^+]}$$ (Eq. A7)

The DIC_{cf} and the aragonite saturation state of the calcifying fluid (Ω_{cf}) were then calculated following D'Olivo and McCulloch (2017).

$$DIC_{cf} = \left[CO_3^{2-}\right]_{cf} \cdot \left(1 + \frac{[H^+]}{K_2} + \frac{[H^+]}{K_1 \cdot K_2}\right)$$ (Eq. A8)

$$\Omega_{cf} = \frac{[CO_3^{2-}]_{cf} \cdot [Ca^{2+}]_{sw}}{K_{sp}}$$ (Eq. A9)

Where $[Ca^{2+}]_{sw}$ = 0.0112 in mol·kg^{-1} for the Mediterranean Sea (McCulloch et al., 2012). The equilibrium constants of dissociation of H_2CO_3 in seawater (K_1, and K_2), and the solubility product of aragonite (K_{sp}) were calculated following Zeebe and Wolf-Gladrow (2001):

$$\log(K_1) = -\left(\frac{3670.7}{T} - 62.008 + 9.7944 \cdot \ln(T) - 0.0118 \cdot S + 0.000116 \cdot S^2\right)$$ (Eq. A10)

$$\log(K_2) = -\left(\frac{1394.7}{T} + 4.777 - 0.0184 \cdot S - 0.000118 \cdot S^2\right)$$ (Eq. A11)

$$\log(K_{sp}) = -171.945 - 0.077993 \cdot T + \frac{2903.293}{T} + 71.595 \cdot \log(T) + \left(-0.068393 + 0.0017276 \cdot T + \frac{88.135}{T}\right) \cdot \sqrt{S} - 0.10018 \cdot S + 0.0059415 \cdot \sqrt{S^3}$$ (Eq. A12)

https://doi.org/10.5194/egusphere-2026-2720
Preprint. Discussion started: 29 May 2026

Appendix B

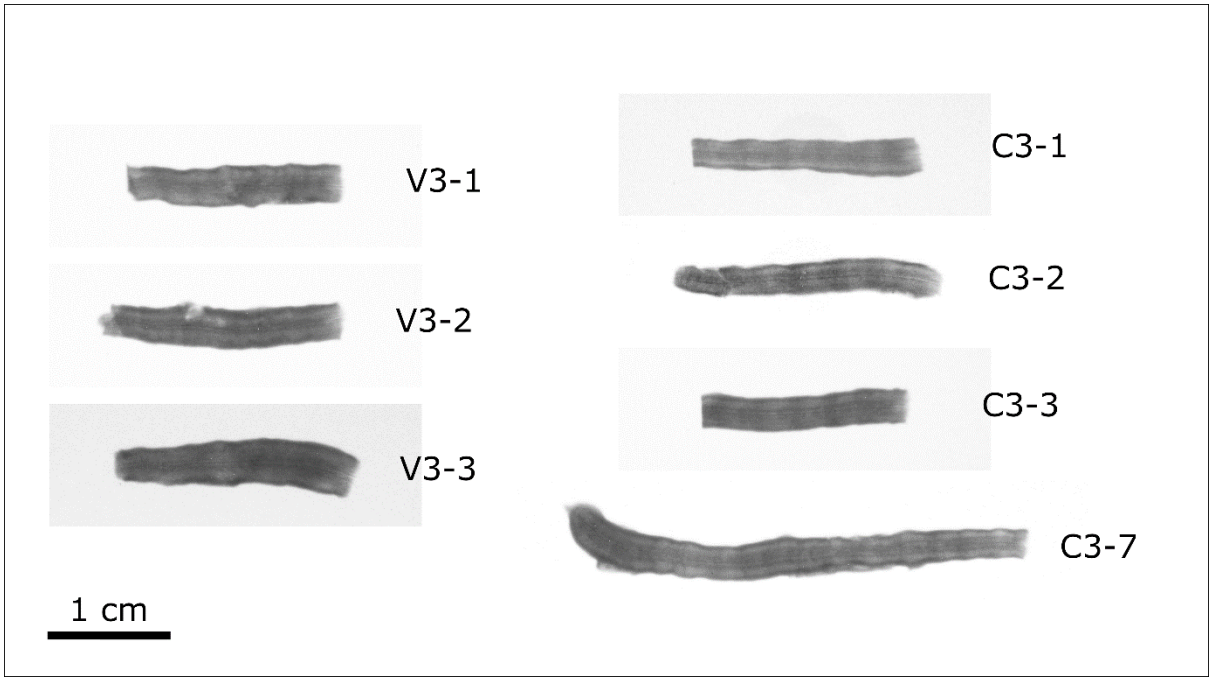

Figure B1. X-ray images of the *Cladocora caespitosa* corallites of this study. All images follow the same scale indicated in the bottom-left corner.

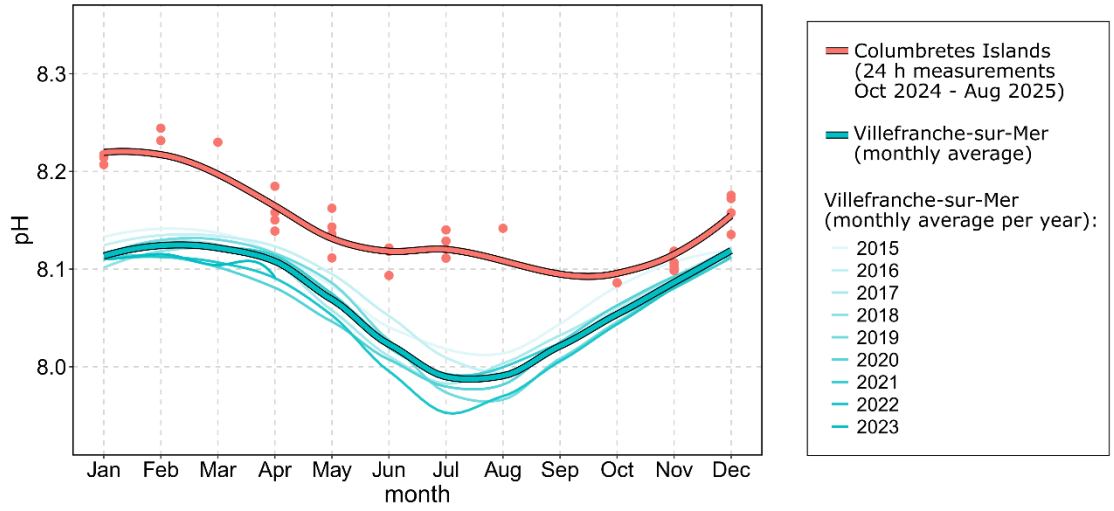

Figure B2. Average monthly pH_{sw} measured at 15 m, continuously throughout the day, in the Columbretes Islands between October 2024 and August 2025 (bold red), and measured at 1 m, at 9:00 LT, in Villefranche between 2007 and 2023 (bold blue), represented using a loess smoothing factor for visualization purposes. For the Columbretes Islands, average weekly values are shown (red dots). Monthly profiles for individual years for Villefranche are also included (thin lines).

https://doi.org/10.5194/egusphere-2026-2720
Preprint. Discussion started: 29 May 2026

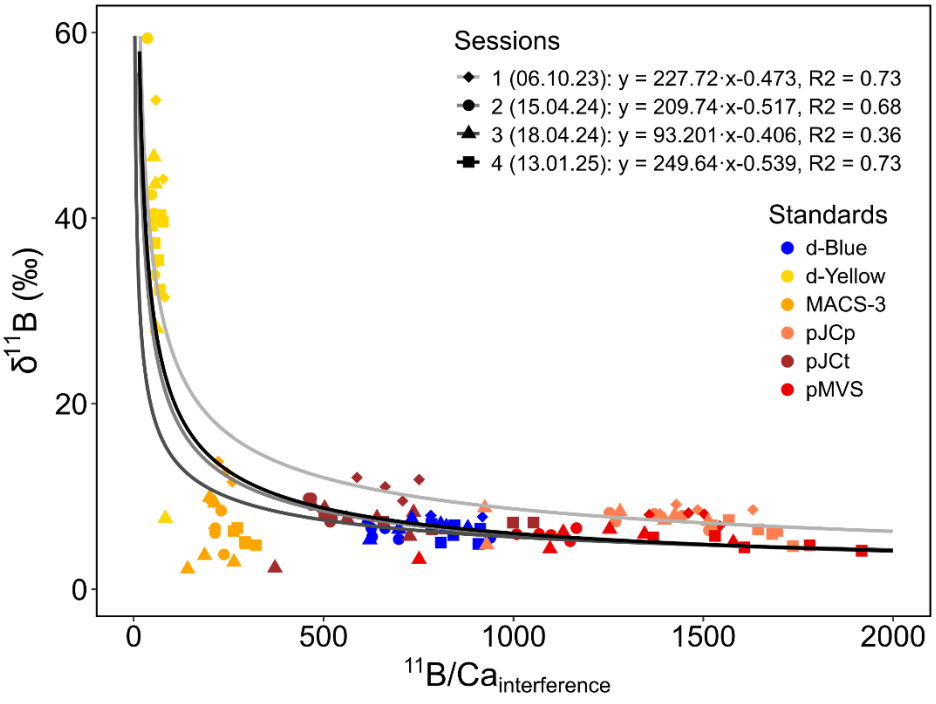

Figure B3. $^{11}B/^{10.066}B$ interference ratio values ($^{11}B/Ca_{interference}$) of standard calibration materials represented against the offset from their true $^{11}B/^{10}B$ values. The standards are differentiated by colour, and each session is differentiated by point shape. A power function regression curve was fitted for each session, and represented using the corresponding shades of grey.

Table B1. Average annual growth parameters and standard deviation (± SD) per sample, calculated between 2013 and 2017 for the Columbretes Islands (n = 4), and between 2015 and 2022 for Villefranche (n = 7).

	Extension ($mm \cdot yr^{-1}$)	Density ($g \cdot cm^{-3} \cdot yr^{-1}$)	Calcification ($g \cdot cm^{-2} \cdot yr^{-1}$)
Columbretes Islands			
C3-1	4.75 ± 0.56	1.12 ± 0.08	0.26 ± 0.02
C3-2	3.71 ± 1.13	1.51 ± 0.11	0.28 ± 0.10
C3-3	4.06 ± 0.19	1.46 ± 0.04	0.30 ± 0.02
C3-7	3.77 ± 0.99	1.32 ± 0.22	0.25 ± 0.10
Villefranche			
V3-1	3.23 ± 0.96	1.11 ± 0.07	0.18 ± 0.05
V3-2	2.76 ± 0.81	1.37 ± 0.06	0.19 ± 0.06
V3-3	3.28 ± 1.17	1.46 ± 0.23	0.24 ± 0.08

https://doi.org/10.5194/egusphere-2026-2720
Preprint. Discussion started: 29 May 2026

Table B2. Typical operating conditions used for each instrument and type of analysis.

Type of analysis	**$\delta^{11}B$**	**Trace elements**		
Samples	**All samples**	**C3-1, C3-2, C3-3, V3-2, V3-3**	**V3-1**	**C3-7**
Laser setup	*In-house custom-built UV 196 nm GFZ Fem2*	*In-house custom-built UV 196 nm GFZ Fem2*	*Analyte Excite Excimer ArF* 193 nm*	*Teledyne Photon Machines Analyte Excite 193 nm ArF excimer*
Energy density ($J \cdot cm^{-2}$)	1-3	1-3	4.56	4
Beam size (µm)	20 (spot)	20 (spot)	155x20 (rectangle)	155x20 (rectangle)
Repetition rate (Hz)	166.7	50	5	10
Scan speed ($\mu m \cdot s^{-1}$)	38	38	10	50
He carrier gas ($L \cdot min^{-1}$)	1.22	0.81	0.65	0.4
Mass spectrometry setup	*Thermo Neptune MC-ICP-MS*	*Thermo Scientific iCAP Quadrupole*	*Thermo Scientific iCAP RQ Quadrupole*	*Thermo ElementXR sector field ICP-MS*
RF Power (W)	1250	1550	1550	1200
Ar cooling gas ($L \cdot min^{-1}$)	15	15	14	16
Ar auxiliary gas ($L \cdot min^{-1}$)	0.7-0.9	0.65	0.8	0.87
Ar nebulizer gas ($L \cdot min^{-1}$)	0.72-1.17	0.51	0.92	0.8

https://doi.org/10.5194/egusphere-2026-2720
Preprint. Discussion started: 29 May 2026

Table B3. $\delta^{11}B$ composition of different reference materials measured by chemical separation. The boron concentration used for the measurements is also indicated ([B]), along with the number of measurements that were run (n).

	[B] (ppb)	$\delta^{11}B \pm 2SD$ (‰)	n
JCp-1	4-15	24.14 ± 0.07	3
AE121	2	19.98 ± 1.88	3
	4	19.60 ± 0.17	3
	10	19.72 ± 0.30	3
	20	19.69 ± 0.22	3
DE-B	45.9	-0.03 ± 0.16*	1
DE-Y	10.5	-18.76 ± 0.36*	1

*With ± 2σ external reproducibility, based on the equation of Ring et al. (2025). The DE-B standard was previously analysed with chemical separation by Coenen et al. (2024a), yielding a value of 0.02 ± 0.41 ‰ (n = 20).

Table B4. $\delta^{11}B$ composition of JCp-1-NP, measured with laser ablation, after applying the same interference correction used for the corals. However, we note that likely due to contamination from non-carbonate phases during the nano-milling procedure, absolute $\delta^{11}B$ values were found to be isotopically lighter than powdered JCp-1.

	$\delta^{11}B \pm 2SD$ (‰)	n
day 1	22.78 ± 1.33	12
day 2	22.09 ± 1.12	12
day 3	22.46 ± 2.41	16
day 4	21.83 ± 1.10	13
Measured via solution	21.99	1

https://doi.org/10.5194/egusphere-2026-2720
Preprint. Discussion started: 29 May 2026

Table B5. Average trace element values per session of JCp-1-NP ± SD, measured with laser ablation.

	Li/Ca ($\mu mol \cdot mol^{-1}$)	B/Ca ($\mu mol \cdot mol^{-1}$)	Mg/Ca ($mmol \cdot mol^{-1}$)	Sr/Ca ($mmol \cdot mol^{-1}$)	n
In-house custom-built UV 196 nm GFZ Fem2 laser ablation system, coupled with Thermo Scientific iCAP Quadrupole					
Session 1	8.19 ± 0.35	355 ± 25	4.64 ± 0.19	9.5 ± 1.6	8
Session 2	7.3 ± 1.1	362 ± 17	4.53 ± 0.26	9.88 ± 0.23	13
Session 3	8.11 ± 0.30	393 ± 24	4.68 ± 0.22	9.33 ± 0.72	10
Session 4	9.7 ± 2.1	323.3 ± 9.2	4.79 ± 0.13	10.5 ± 2.0	7
Analyte Excite Excimer ArF 193 nm laser ablation system, coupled with Thermo Scientific iCAP RQ Quadrupole*					
Session 1	14.6 ± 1.2	546 ± 25	4.21 ± 0.14	10.29 ± 0.75	18
Teledyne Photon Machines Analyte Excite 193 nm ArF excimer laser ablation system, coupled with Thermo ElementXR sector field ICP-MS					
Session 1	7.8 ± 3.4	289 ± 31	3.45 ± 0.18	10.16 ± 0.32	6
Published values for JCp-1 (Hathorne et al., 2013) *(robust average ± robust standard deviation)*					
	6.185 ± 0.107	459.6 ± 22.7	4.199 ± 0.065	8.838 ± 0.042	21

https://doi.org/10.5194/egusphere-2026-2720
Preprint. Discussion started: 29 May 2026

Table B6. Average geochemical parameters and standard deviation (± SD) calculated per coral sample. Each coral sample included 40 measurements.

	$\delta^{11}B$ (‰)	B/Ca ($\mu mol \cdot mol^{-1}$)	pH_{cf}	pH_{sw}	DIC_{cf} ($\mu mol \cdot kg^{-1}$)	Ω_{cf}
Columbretes Islands						
C3-1	24.15 ± 0.85	683 ± 59	8.55 ± 0.07	7.81 ± 0.14	3437 ± 292	13.6 ± 1.7
C3-2	24.7 ± 1.2	703 ± 89	8.59 ± 0.10	7.90 ± 0.20	3342 ± 453	13.8 ± 2.0
C3-3	24.5 ± 1.1	695 ± 53	8.58 ± 0.10	7.88 ± 0.20	3370 ± 253	13.6 ± 1.5
C3-7	25.05 ± 0.96	695 ± 38	8.61 ± 0.10	7.95 ± 0.21	3292 ± 204	14.19 ± 0.73
average	24.6 ± 1.1	694 ± 62	8.58 ± 0.09	7.88 ± 0.20	3358 ± 314	13.8 ± 1.5
Villefranche						
V3-1	26.04 ± 0.98	785 ± 66	8.69 ± 0.10	8.11 ± 0.20	2859 ± 230	13.6 ± 1.4
V3-2	25.34 ± 0.84	778 ± 58	8.65 ± 0.08	8.01 ± 0.16	2938 ± 223	13.0 ± 1.0
V3-3	25.67 ± 0.89	785 ± 64	8.66 ± 0.09	8.04 ± 0.18	2873 ± 210	13.2 ± 1.3
average	25.68 ± 0.94	782 ± 62	8.67 ± 0.09	8.06 ± 0.19	2892 ± 222	13.3 ± 1.2

https://doi.org/10.5194/egusphere-2026-2720
Preprint. Discussion started: 29 May 2026

Table B7. Summary of the ANOVA between sites, using the seasonal coral growth, monthly geochemical compositions and carbonate parameters per sample and, and weekly *in situ* temperatures of Villefranche and the Columbretes Islands.

Variables	DF	F-Value	p-Value
Growth parameters			
Linear extension	1, 72	13.40	<0.001
Skeletal density	1, 72	0.541	0.465
Calcification	1, 72	13.23	<0.001
Geochemical parameters			
$\delta^{11}B$	1, 242	74.31	<0.001
B/Ca	1, 242	120.5	<0.001
DIC_{cf}	1, 242	167.7	<0.001
Ω_{cf}	1, 242	8.16	0.005
pH_{cf}	1, 242	48.69	<0.001

9 Data availability

The data that support the findings of this study are available in the Zenodo online repository https://doi.org/10.5281/zenodo.18248853 (Vergotti et al., 2026), and the GFZ data repository doi:10.5880/fidgeo.2025.094 (Vergotti et al., 2025a).

10 Author contribution

Marina J. Vergotti, Diego K. Kersting and Juan Pablo D'Olivo conceived the ideas behind this study. Marina J. Vergotti, Michael J. Henehan, Daniel Frick, Josefine Holtz, and Valby van Schijndel produced the data at the GFZ Helmholtz Centre for Geosciences (Potsdam, Germany). Diego K. Kersting and Ed C. Hathorne produced the data at the GEOMAR Helmholtz Centre for Ocean Research (Kiel, Germany). Marina J. Vergotti, Daniel Frick, Ed C. Hathorne, Michael J. Henehan, Josefine Holtz, Juan Pablo D'Olivo, Diego K. Kersting and Valby van Schijndel carried out the data evaluation and analyses. Diego K. Kersting and Juan Pablo D'Olivo supervised the findings of this work. Steeve Comeau and Núria Teixidó contributed with

https://doi.org/10.5194/egusphere-2026-2720
Preprint. Discussion started: 29 May 2026

temperature data and coral samples from Villefranche. Thomas C. Brachert contributed with guidance, materials and methods to obtain the X-ray images. Marina J. Vergotti took the lead in writing the manuscript, and all coauthors provided critical feedback and helped shape the manuscript.

11 Competing interests

The authors declare that they have no conflict of interest.

12 Acknowledgments

We thank the Secretaría General de Pesca (MAPA) and the Columbretes Islands Marine Reserve staff for sampling authorization and logistic support in the gathering of biological and environmental data. We thank Dr. J.E. Hoffmann for giving us access to the micro-mill. We thank Dr. B. Chen, Dr. S. Ring and A. Balduin for their support in the lab, and J. Bernebee-Sey for his assistance in processing the data. We thank G.O. Cardoso for insightful conversations and early manuscript readings and comments.

References

Al-Horani, F. A., Al-Moghrabi, S. M., and de Beer, D.: The mechanism of calcification and its relation to photosynthesis and respiration in the scleractinian coral Galaxea fascicularis, Mar. Biol., 142, 419–426, https://doi.org/10.1007/s00227-002-0981-8, 2003.

Bates, D., Mächler, M., Bolker, B., and Walker, S.: Fitting Linear Mixed-Effects Models Using lme4, J. Stat. Softw., 67, 1–48, https://doi.org/10.18637/jss.v067.i01, 2014.

Bernardet, C., Tambutté, E., Techer, N., Tambutté, S., and Venn, A. A.: Ion transporter gene expression is linked to the thermal sensitivity of calcification in the reef coral Stylophora pistillata, Sci. Rep., 9, 18676, https://doi.org/10.1038/s41598-019-54814-7, 2019.

Canesi, M., Douville, E., Montagna, P., Taviani, M., Stolarski, J., Bordier, L., Dapoigny, A., Coulibaly, G. E. H., Simon, A.-C., Agelou, M., Fin, J., Metzl, N., Iwankow, G., Allemand, D., Planes, S., Moulin, C., Lombard, F., Bourdin, G., Troublé, R., Agostini, S., Banaigs, B., Boissin, E., Boss, E., Bowler, C., de Vargas, C., Flores, M., Forcioli, D., Furla, P., Gilson, E., Galand, P. E., Pesant, S., Sunagawa, S., Thomas, O. P., Vega Thurber, R., Voolstra, C. R., Wincker, P., Zoccola, D., and Reynaud, S.: Differences in carbonate chemistry up-regulation of long-lived reef-building corals, Sci. Rep., 13, 11589, https://doi.org/10.1038/s41598-023-37598-9, 2023.

Canesi, M., Douville, É., Bordier, L., Dapoigny, A., Coulibaly, G. E., Montagna, P., Béraud, É., Allemand, D., Planes, S., Furla, P., Gilson, E., Roberty, S., Zoccola, D., and Reynaud, S.: Porites' coral calcifying fluid chemistry regulation under normal- and low-pH seawater conditions in Palau Archipelago: Impacts on growth properties, Sci. Total Environ., 911, 168552, https://doi.org/10.1016/j.scitotenv.2023.168552, 2024.

https://doi.org/10.5194/egusphere-2026-2720
Preprint. Discussion started: 29 May 2026

Carbonne, C., Teixidó, N., Moore, B., Mirasole, A., Guttierez, T., Gattuso, J.-P., and Comeau, S.: Two temperate corals are tolerant to low pH regardless of previous exposure to natural CO2 vents, Limnol. Oceanogr., 66, 4046–4061, https://doi.org/10.1002/lno.11942, 2021.

Casado-Amezúa, P., Kersting, D., Linares, C. L., Bo, M., Caroselli, E., Garrabou, J., Cerrano, C., Ozalp, B., Terrón-Sigler, A., and Betti, F.: IUCN Red List of Threatened Species: Cladocora caespitosa, IUCN Red List Threat. Species, 28, http://dx.doi.org/10.2305/IUCN.UK.2015- 2.RLTS.T133142A75872554.en, 2015.

Chalk, T. B., Standish, C. D., D'Angelo, C., Castillo, K. D., Milton, J. A., and Foster, G. L.: Mapping coral calcification strategies from in situ boron isotope and trace element measurements of the tropical coral Siderastrea siderea, Sci. Rep., 11, 472, https://doi.org/10.1038/s41598-020-78778-1, 2021.

Chen, X., D'Olivo, J. P., Wei, G., and McCulloch, M.: Anthropogenic ocean warming and acidification recorded by Sr/Ca, Li/Mg, δ11B and B/Ca in Porites coral from the Kimberley region of northwestern Australia, Palaeogeogr. Palaeoclimatol. Palaeoecol., 528, 50–59, https://doi.org/10.1016/j.palaeo.2019.04.033, 2019.

Coenen, D., Evans, D., Hauzer, H., Nambiar, R., Jurikova, H., Dumont, M., Kanna, P., Rae, J., Erez, J., Cotton, L., Renema, W., and Müller, W.: Boron isotope pH calibration of a shallow dwelling benthic nummulitid foraminifera, Geochim. Cosmochim. Acta, 378, 217–233, https://doi.org/10.1016/j.gca.2024.06.020, 2024a.

Coenen, D., Evans, D., Jurikova, H., Dumont, M., Rae, J., and Müller, W.: Determining the sources of (sub)permil-level inaccuracy during laser ablation-MC-ICPMS boron isotope measurements of carbonates, J. Anal. At. Spectrom., 39, 2409–2420, https://doi.org/10.1039/D4JA00154K, 2024b.

Cohen, A. L. and McConnaughey, T. A.: Geochemical Perspectives on Coral Mineralization, Rev. Mineral. Geochem., 54, 151–187, https://doi.org/10.2113/0540151, 2003.

Coma, R., Ribes, M., Serrano, E., Jiménez, E., Salat, J., and Pascual, J.: Global warming-enhanced stratification and mass mortality events in the Mediterranean, Proc. Natl. Acad. Sci., 106, 6176–6181, https://doi.org/10.1073/pnas.0805801106, 2009.

Comeau, S., Edmunds, P. J., Spindel, N. B., and Carpenter, R. C.: Fast coral reef calcifiers are more sensitive to ocean acidification in short-term laboratory incubations, Limnol. Oceanogr., 59, 1081–1091, https://doi.org/10.4319/lo.2014.59.3.1081, 2014.

Comeau, S., Tambutté, E., Carpenter, R. C., Edmunds, P. J., Evensen, N. R., Allemand, D., Ferrier-Pagès, C., Tambutté, S., and Venn, A. A.: Coral calcifying fluid pH is modulated by seawater carbonate chemistry not solely seawater pH, Proc. R. Soc. B Biol. Sci., 284, 20161669, https://doi.org/10.1098/rspb.2016.1669, 2017a.

Comeau, S., Cornwall, C. E., and McCulloch, M. T.: Decoupling between the response of coral calcifying fluid pH and calcification to ocean acidification, Sci. Rep., 7, 7573, https://doi.org/10.1038/s41598-017-08003-z, 2017b.

Comeau, S., Cornwall, C. E., Pupier, C. A., DeCarlo, T. M., Alessi, C., Trehern, R., and McCulloch, M. T.: Flow-driven micro-scale pH variability affects the physiology of corals and coralline algae under ocean acidification, Sci. Rep., 9, 12829, https://doi.org/10.1038/s41598-019-49044-w, 2019a.

Comeau, S., Cornwall, C. E., DeCarlo, T. M., Doo, S. S., Carpenter, R. C., and McCulloch, M. T.: Resistance to ocean acidification in coral reef taxa is not gained by acclimatization, Nat. Clim. Change, 9, 477–483, https://doi.org/10.1038/s41558-019-0486-9, 2019b.

https://doi.org/10.5194/egusphere-2026-2720
Preprint. Discussion started: 29 May 2026

Darmaraki, S.: Mediterranean marine heatwaves : detection, past variability and future evolution, PhD Thesis, Université Paul Sabatier - Toulouse III, 2019.

Dissard, D., Douville, E., Reynaud, S., Juillet-Leclerc, A., Montagna, P., Louvat, P., and McCulloch, M.: Light and temperature effects on δ11B and B/Ca ratios of the zooxanthellate coral Acropora sp.: results from culturing experiments, Biogeosciences, 9, 4589–4605, https://doi.org/10.5194/bg-9-4589-2012, 2012.

D'Olivo, J. P. and McCulloch, M. T.: Response of coral calcification and calcifying fluid composition to thermally induced bleaching stress, Sci. Rep., 7, 2207, https://doi.org/10.1038/s41598-017-02306-x, 2017.

D'Olivo, J. P., Ellwood, G., DeCarlo, T. M., and McCulloch, M. T.: Deconvolving the long-term impacts of ocean acidification and warming on coral biomineralisation, Earth Planet. Sci. Lett., 526, 115785, https://doi.org/10.1016/j.epsl.2019.115785, 2019a.

D'Olivo, J. P., Georgiou, L., Falter, J., DeCarlo, T. M., Irigoien, X., Voolstra, C. R., Roder, C., Trotter, J., and McCulloch, M. T.: Long-Term Impacts of the 1997–1998 Bleaching Event on the Growth and Resilience of Massive Porites Corals From the Central Red Sea, Geochem. Geophys. Geosystems, 20, 2936–2954, https://doi.org/10.1029/2019GC008312, 2019b.

Evans, D., Gerdes, A., Coenen, D., Marschall, H. R., and Müller, W.: Accurate correction for the matrix interference on laser ablation MC-ICPMS boron isotope measurements in CaCO3 and silicate matrices, J. Anal. At. Spectrom., 36, 1607–1617, https://doi.org/10.1039/D1JA00073J, 2021.

Foster, G. L.: Seawater pH, pCO2 and [CO2−3] variations in the Caribbean Sea over the last 130 kyr: A boron isotope and B/Ca study of planktic foraminifera, Earth Planet. Sci. Lett., 271, 254–266, https://doi.org/10.1016/j.epsl.2008.04.015, 2008.

Foster, G. L. and Rae, J. W. B.: Reconstructing Ocean pH with Boron Isotopes in Foraminifera, Annu. Rev. Earth Planet. Sci., 44, 207–237, https://doi.org/10.1146/annurev-earth-060115-012226, 2016.

Fowell, S. E., Foster, G. L., Ries, J. B., Castillo, K. D., de la Vega, E., Tyrrell, T., Donald, H. K., and Chalk, T. B.: Historical Trends in pH and Carbonate Biogeochemistry on the Belize Mesoamerican Barrier Reef System, Geophys. Res. Lett., 45, 3228–3237, https://doi.org/10.1002/2017GL076496, 2018.

Fox, J. and Weisberg, S.: An R companion to applied regression, 3rd ed., Sage publications, 2018.

Furla, P., Galgani, I., Durand, I., and Allemand, D.: Sources and Mechanisms of Inorganic Carbon Transport for Coral Calcification and Photosynthesis, J. Exp. Biol., 203, 3445–3457, https://doi.org/10.1242/jeb.203.22.3445, 2000.

Garrabou, J., Gómez-Gras, D., Medrano, A., Cerrano, C., Ponti, M., Schlegel, R., Bensoussan, N., Turicchia, E., Sini, M., Gerovasileiou, V., Teixido, N., Mirasole, A., Tamburello, L., Cebrian, E., Rilov, G., Ledoux, J.-B., Souissi, J. B., Khamassi, F., Ghanem, R., Benabdi, M., Grimes, S., Ocaña, O., Bazairi, H., Hereu, B., Linares, C., Kersting, D. K., la Rovira, G., Ortega, J., Casals, D., Pagès-Escolà, M., Margarit, N., Capdevila, P., Verdura, J., Ramos, A., Izquierdo, A., Barbera, C., Rubio-Portillo, E., Anton, I., López-Sendino, P., Díaz, D., Vázquez-Luis, M., Duarte, C., Marbà, N., Aspillaga, E., Espinosa, F., Grech, D., Guala, I., Azzurro, E., Farina, S., Cristina Gambi, M., Chimienti, G., Montefalcone, M., Azzola, A., Mantas, T. P., Fraschetti, S., Ceccherelli, G., Kipson, S., Bakran-Petricioli, T., Petricioli, D., Jimenez, C., Katsanevakis, S., Kizilkaya, I. T., Kizilkaya, Z., Sartoretto, S., Elodie, R., Ruitton, S., Comeau, S., Gattuso, J.-P., and Harmelin, J.-G.: Marine heatwaves drive recurrent mass mortalities in the Mediterranean Sea, Glob. Change Biol., 28, 5708–5725, https://doi.org/10.1111/gcb.16301, 2022.

Gattuso, J.-P., Allemand, D., and Frankignoulle, M.: Photosynthesis and Calcification at Cellular, Organismal and Community Levels in Coral Reefs: A Review on Interactions and Control by Carbonate Chemistry, Am. Zool., 39, 160–183, https://doi.org/10.1093/icb/39.1.160, 1999.

https://doi.org/10.5194/egusphere-2026-2720
Preprint. Discussion started: 29 May 2026

Gattuso, J.-P., Magnan, A., Billé, R., Cheung, W. W. L., Howes, E. L., Joos, F., Allemand, D., Bopp, L., Cooley, S. R., Eakin, C. M., Hoegh-Guldberg, O., Kelly, R. P., Pörtner, H.-O., Rogers, A. D., Baxter, J. M., Laffoley, D., Osborn, D., Rankovic, A., Rochette, J., Sumaila, U. R., Treyer, S., and Turley, C.: Contrasting futures for ocean and society from different anthropogenic CO2 emissions scenarios, Science, 349, aac4722, https://doi.org/10.1126/science.aac4722, 2015a.

Gattuso, J.-P., Epitalon, J.-M., Lavigne, H., Orr, J., Gentili, B., Hagens, M., Hofmann, A., Mueller, J.-D., Proye, A., and Rae, J.: Package 'seacarb,' Prepr. Httpcran R-Proj. Orgpackage Seacarb, 2015b.

Gattuso, J.-P., Alliouane, S., and Mousseau, L.: Seawater carbonate chemistry in the Bay of Villefranche, Point B (France), January 2007 - June 2023, https://doi.org/10.1594/PANGAEA.727120, 2021.

Geri, P., El Yacoubi, S., and Goyet, C.: Forecast of Sea Surface Acidification in the Northwestern Mediterranean Sea, J. Comput. Environ. Sci., 2014, 1–7, https://doi.org/10.1155/2014/201819, 2014.

Guo, W.: Seawater temperature and buffering capacity modulate coral calcifying pH, Sci. Rep., 9, 1189, https://doi.org/10.1038/s41598-018-36817-y, 2019.

Hassoun, A. E. R., Bantelman, A., Canu, D., Comeau, S., Galdies, C., Gattuso, J.-P., Giani, M., Grelaud, M., Hendriks, I. E., Ibello, V., Idrissi, M., Krasakopoulou, E., Shaltout, N., Solidoro, C., Swarzenski, P. W., and Ziveri, P.: Ocean acidification research in the Mediterranean Sea: Status, trends and next steps, Front. Mar. Sci., 9, https://doi.org/10.3389/fmars.2022.892670, 2022.

Hassoun, A. E. R., Mojtahid, M., Merheb, M., Lionello, P., Gattuso, J.-P., and Cramer, W.: Climate change risks on key open marine and coastal mediterranean ecosystems, Sci. Rep., 15, 24907, https://doi.org/10.1038/s41598-025-07858-x, 2025.

Hathorne, E. C., Gagnon, A., Felis, T., Adkins, J., Asami, R., Boer, W., Caillon, N., Case, D., Cobb, K. M., Douville, E., deMenocal, P., Eisenhauer, A., Garbe-Schönberg, D., Geibert, W., Goldstein, S., Hughen, K., Inoue, M., Kawahata, H., Kölling, M., Cornec, F. L., Linsley, B. K., McGregor, H. V., Montagna, P., Nurhati, I. S., Quinn, T. M., Raddatz, J., Rebaubier, H., Robinson, L., Sadekov, A., Sherrell, R., Sinclair, D., Tudhope, A. W., Wei, G., Wong, H., Wu, H. C., and You, C.-F.: Interlaboratory study for coral Sr/Ca and other element/Ca ratio measurements, Geochem. Geophys. Geosystems, 14, 3730–3750, https://doi.org/10.1002/ggge.20230, 2013.

Hemming, N. G. and Hanson, G. N.: Boron isotopic composition and concentration in modern marine carbonates, Geochim. Cosmochim. Acta, 56, 537–543, https://doi.org/10.1016/0016-7037(92)90151-8, 1992.

Holcomb, M., Venn, A. A., Tambutté, E., Tambutté, S., Allemand, D., Trotter, J., and McCulloch, M.: Coral calcifying fluid pH dictates response to ocean acidification, Sci. Rep., 4, 5207, https://doi.org/10.1038/srep05207, 2014.

Holcomb, M., DeCarlo, T. M., Gaetani, G. A., and McCulloch, M.: Factors affecting B/Ca ratios in synthetic aragonite, Chem. Geol., 437, 67–76, https://doi.org/10.1016/j.chemgeo.2016.05.007, 2016.

Hönisch, B., Hemming, N. G., Grottoli, A. G., Amat, A., Hanson, G. N., and Bijma, J.: Assessing scleractinian corals as recorders for paleo-pH: Empirical calibration and vital effects, Geochim. Cosmochim. Acta, 68, 3675–3685, https://doi.org/10.1016/j.gca.2004.03.002, 2004.

Hoogenboom, M., Rodolfo-Metalpa, R., and Ferrier-Pages, C.: Co-variation between autotrophy and heterotrophy in the Mediterranean coral Cladocora caespitosa, J. Exp. Biol., 213, 2399–2409, https://doi.org/10.1242/jeb.040147, 2010.

https://doi.org/10.5194/egusphere-2026-2720
Preprint. Discussion started: 29 May 2026

Hulver, A. M., Teixidó, N., Kemp, D. W., Keister, E. F., Gattuso, J.-P., and Grottoli, A. G.: High heterotrophic capacity favors Mediterranean coral success and resilience in the face of ocean acidification, Coral Reefs, 44, 1041–1054, https://doi.org/10.1007/s00338-025-02663-4, 2025.

Inoue, M., Nohara, M., Okai, T., Suzuki, A., and Kawahata, H.: Concentrations of Trace Elements in Carbonate Reference Materials Coral JCp-1 and Giant Clam JCt-1 by Inductively Coupled Plasma-Mass Spectrometry, Geostand. Geoanalytical Res., 28, 411–416, https://doi.org/10.1111/j.1751-908X.2004.tb00759.x, 2004.

IPCC: IPCC special report on the ocean and cryosphere in a changing climate [H.-O. Pörtner, D. C. Roberts, V. Masson-Delmotte, P. Zhai, M. Tignor, E. Poloczanska, K. Mintenbeck, A. Alegría, M. Nicolai, A. Okem, J. Petzold, B. Rama, & N. M. Weyer (Eds.)]., Cambridge University Press, Cambridge, UK, 2019.

Jochum, K. P., Weis, U., Stoll, B., Kuzmin, D., Yang, Q., Raczek, I., Jacob, D. E., Stracke, A., Birbaum, K., Frick, D. A., Günther, D., and Enzweiler, J.: Determination of Reference Values for NIST SRM 610–617 Glasses Following ISO Guidelines, Geostand. Geoanalytical Res., 35, 397–429, https://doi.org/10.1111/j.1751-908X.2011.00120.x, 2011.

Jochum, K. P., Scholz, D., Stoll, B., Weis, U., Wilson, S. A., Yang, Q., Schwalb, A., Börner, N., Jacob, D. E., and Andreae, M. O.: Accurate trace element analysis of speleothems and biogenic calcium carbonates by LA-ICP-MS, Chem. Geol., 318–319, 31–44, https://doi.org/10.1016/j.chemgeo.2012.05.009, 2012.

Jochum, K. P., Garbe-Schönberg, D., Veter, M., Stoll, B., Weis, U., Weber, M., Lugli, F., Jentzen, A., Schiebel, R., Wassenburg, J. A., Jacob, D. E., and Haug, G. H.: Nano-Powdered Calcium Carbonate Reference Materials: Significant Progress for Microanalysis?, Geostand. Geoanalytical Res., 43, 595–609, https://doi.org/10.1111/ggr.12292, 2019.

Jurikova, H., Ippach, M., Liebetrau, V., Gutjahr, M., Krause, S., Büsse, S., Gorb, S. N., Henkel, D., Hiebenthal, C., Schmidt, M., Leipe, T., Laudien, J., and Eisenhauer, A.: Incorporation of minor and trace elements into cultured brachiopods: Implications for proxy application with new insights from a biomineralisation model, Geochim. Cosmochim. Acta, 286, 418–440, https://doi.org/10.1016/j.gca.2020.07.026, 2020.

Kang, H., Chen, X., Deng, W., Chen, T., Cai, G., and Wei, G.: Imprints of Atlantic Multidecadal Oscillation on pantropical seawater pH inferred from coral δ11B records, Quat. Sci. Rev., 344, https://doi.org/10.1016/j.quascirev.2024.109003, 2024.

Kapsenberg, L., Alliouane, S., Gazeau, F., Mousseau, L., and Gattuso, J.-P.: Coastal ocean acidification and increasing total alkalinity in the northwestern Mediterranean Sea, Ocean Sci., 13, 411–426, https://doi.org/10.5194/os-13-411-2017, 2017.

Kersting, D. K. and Linares, C.: Cladocora caespitosa bioconstructions in the Columbretes Islands Marine Reserve (Spain, NW Mediterranean): distribution, size structure and growth: Cladocora caespitosa bioconstructions in the Columbretes Islands Marine Reserve, Mar. Ecol., 33, 427–436, https://doi.org/10.1111/j.1439-0485.2011.00508.x, 2012.

Kersting, D. K., Bensoussan, N., and Linares, C.: Long-Term Responses of the Endemic Reef-Builder Cladocora caespitosa to Mediterranean Warming, PLoS ONE, 8, e70820, https://doi.org/10.1371/journal.pone.0070820, 2013.

Kersting, D. K., Cebrian, E., Casado, C., Teixidó, N., Garrabou, J., and Linares, C.: Experimental evidence of the synergistic effects of warming and invasive algae on a temperate reef-builder coral, Sci. Rep., 5, 18635, https://doi.org/10.1038/srep18635, 2015.

Kersting, D. K., Cebrian, E., Verdura, J., and Ballesteros, E.: A new Cladocora caespitosa population with unique ecological traits, Mediterr. Mar. Sci., 18, 38, https://doi.org/10.12681/mms.1955, 2017.

https://doi.org/10.5194/egusphere-2026-2720
Preprint. Discussion started: 29 May 2026

Kersting, D. K., Casado-Amezua, P., and Goffredo, S.: Cladocora caespitosa, IUCN Red List Threat. Species, e.T133142A165739749., 2022.

Kersting, D. K., Cefalì, M. E., Movilla, J., Vergotti, M. J., and Linares, C.: The endangered coral Cladocora caespitosa in the Menorca Biosphere Reserve: Distribution, demographic traits and threats, Ocean Coast. Manag., 240, 106626, https://doi.org/10.1016/j.ocecoaman.2023.106626, 2023.

Kersting, D. K., Brachert, T. C., D'Olivo, J. P., Linares, C., Reuning, L., Riera, J. L., Spreter, P., Struck, U., Vergotti, M. J., and Zinke, J.: High-resolution coral oxygen and carbon isotope records reveal temperature and autotrophy dynamics in a Mediterranean climate change hotspot, Limnol. Oceanogr., n/a, https://doi.org/10.1002/lno.70208, 2025.

Kleypas, J. A., Feely, R. A., Fabry, V. J., Langdon, C., Sabine, C. L., and Robbins, L. L.: Impacts of Ocean Acidification on Coral Reefs and Other Marine Calcifiers: A Guide for Future Research: a Report from a Workshop Sponsored by the National Science Foundation, the National Oceanic and Atmospheric Administration, and the US Geological Survey, University Corporation for Atmospheric Research, 2006.

Klochko, K., Kaufman, A. J., Yao, W., Byrne, R. H., and Tossell, J. A.: Experimental measurement of boron isotope fractionation in seawater, Earth Planet. Sci. Lett., 248, 276–285, https://doi.org/10.1016/j.epsl.2006.05.034, 2006.

Knebel, O., Carvajal, C., Standish, C. D., Vega, E. de la, Chalk, T. B., Ryan, E. J., Guo, W., Ford, M., Foster, G. L., and Kench, P.: Porites Calcifying Fluid pH on Seasonal to Diurnal Scales, J. Geophys. Res. Oceans, 126, e2020JC016889, https://doi.org/10.1029/2020JC016889, 2021.

Krief, S., Hendy, E. J., Fine, M., Yam, R., Meibom, A., Foster, G. L., and Shemesh, A.: Physiological and isotopic responses of scleractinian corals to ocean acidification, Geochim. Cosmochim. Acta, 74, 4988–5001, https://doi.org/10.1016/j.gca.2010.05.023, 2010.

Kružić, P. and Benković, L.: Bioconstructional features of the coral Cladocora caespitosa (Anthozoa, Scleractinia) in the Adriatic Sea (Croatia), Mar. Ecol., 29, 125–139, https://doi.org/10.1111/j.1439-0485.2008.00220.x, 2008.

Kružić, P., Sršen, P., and Benković, L.: The impact of seawater temperature on coral growth parameters of the colonial coral Cladocora caespitosa (Anthozoa, Scleractinia) in the eastern Adriatic Sea, Facies, 58, 477–491, https://doi.org/10.1007/s10347-012-0306-4, 2012.

Kwiatkowski, L., Torres, O., Bopp, L., Aumont, O., Chamberlain, M., Christian, J. R., Dunne, J. P., Gehlen, M., Ilyina, T., John, J. G., Lenton, A., Li, H., Lovenduski, N. S., Orr, J. C., Palmieri, J., Santana-Falcón, Y., Schwinger, J., Séférian, R., Stock, C. A., Tagliabue, A., Takano, Y., Tjiputra, J., Toyama, K., Tsujino, H., Watanabe, M., Yamamoto, A., Yool, A., and Ziehn, T.: Twenty-first century ocean warming, acidification, deoxygenation, and upper-ocean nutrient and primary production decline from CMIP6 model projections, Biogeosciences, 17, 3439–3470, https://doi.org/10.5194/bg-17-3439-2020, 2020.

Liland, K. H., Mevik, B.-H., Wehrens, R., and Hiemstra, P.: pls: Partial Least Squares and Principal Component Regression, 2024.

Lüdecke, D., Ben-Shachar, M. S., Patil, I., Waggoner, P., and Makowski, D.: performance: An R package for assessment, comparison and testing of statistical models, J. Open Source Softw., 6, 3139, https://doi.org/10.21105/joss.03139, 2021.

Martínez, J., Leonelli, F. E., García-Ladona, E., Garrabou, J., Kersting, D. K., Bensoussan, N., and Pisano, A.: Evolution of marine heatwaves in warming seas: the Mediterranean Sea case study, Front. Mar. Sci., 10, https://doi.org/10.3389/fmars.2023.1193164, 2023.

https://doi.org/10.5194/egusphere-2026-2720
Preprint. Discussion started: 29 May 2026

McCulloch, M., Falter, J., Trotter, J., and Montagna, P.: Coral resilience to ocean acidification and global warming through pH up-regulation, Nat. Clim. Change, 2, 623–627, https://doi.org/10.1038/nclimate1473, 2012.

McCulloch, M. T., D'Olivo, J. P., Falter, J., Holcomb, M., and Trotter, J. A.: Coral calcification in a changing World and the interactive dynamics of pH and DIC upregulation, Nat. Commun., 8, 15686, https://doi.org/10.1038/ncomms15686, 2017.

Montagna, P., McCulloch, M., Mazzoli, C., Silenzi, S., and Odorico, R.: The non-tropical coral Cladocora caespitosa as the new climate archive for the Mediterranean: high-resolution (~weekly) trace element systematics, Quat. Sci. Rev., 26, 441–462, https://doi.org/10.1016/j.quascirev.2006.09.008, 2007.

Morri, C., Peirano, A., Bianchi, C. N., and Sassarini, M.: Present-day bioconstructions of the hard coral, Cladocora caespitosa (L.)(Anthozoa, Scleractinia), in the eastern Ligurian Sea (NW Mediterranean), Biol. Mar. Mediterr., 1, 371–372, 1994.

Mousseau, L., Larvor, C., Domeau, A., Durozier, M., Passafiume, O., Laus, C., Petit, F., and De Lary, H.: SO RadeHydro-Point B time series : monitoring a fixed point in a coastal ecosystem, bay of Villefranche sur mer, Ligurian Sea (Western Mediterranean), https://doi.org/10.17882/100175, 2024.

Movilla, J., Calvo, E., Pelejero, C., Coma, R., Serrano, E., Fernández-Vallejo, P., and Ribes, M.: Calcification reduction and recovery in native and non-native Mediterranean corals in response to ocean acidification, J. Exp. Mar. Biol. Ecol., 438, 144–153, https://doi.org/10.1016/j.jembe.2012.09.014, 2012.

Okai, T., Suzuki, A., Kawahata, H., Terashima, S., and Imai, N.: Preparation of a New Geological Survey of Japan Geochemical Reference Material: Coral JCp-1, Geostand. Newsl., 26, 95–99, https://doi.org/10.1111/j.1751-908X.2002.tb00627.x, 2002.

Pandolfi, J. M., Connolly, S. R., Marshall, D. J., and Cohen, A. L.: Projecting Coral Reef Futures Under Global Warming and Ocean Acidification, Science, 333, 418–422, https://doi.org/10.1126/science.1204794, 2011.

Paton, C., Hellstrom, J., Paul, B., Woodhead, J., and Hergt, J.: Iolite: Freeware for the visualisation and processing of mass spectrometric data, J. Anal. At. Spectrom., 26, 2508–2518, https://doi.org/10.1039/C1JA10172B, 2011.

Pearse, V. B.: Incorporation of Metabolic CO2 into Coral Skeleton, Nature, 228, 383–383, https://doi.org/10.1038/228383a0, 1970.

Peirano, A., Morri, C., Mastronuzzi, G., and Bianchi, C. N.: The coral Cladocora caespitosa (Anthozoa, Scleractinia) as a bioherm builder in the Mediterranean Sea, Mem Descr Carta Geol D'It, 52, 59–74, 1998.

Peirano, A., Morri, C., Bianchi, C. N., and Rodolfo-Metalpa, R.: Biomass, carbonate standing stock and production of the mediterranean coral Cladocora caespitosa (L.), Facies, 44, 75–80, https://doi.org/10.1007/BF02668168, 2001.

Peirano, A., Abbate, M., Cerrati, G., Difesca, V., Peroni, C., and Rodolfo-Metalpa, R.: Monthly variations in calix growth, polyp tissue, and density banding of the Mediterranean scleractinian Cladocora caespitosa (L.), Coral Reefs, 24, 404–409, https://doi.org/10.1007/s00338-005-0020-6, 2005.

Pinheiro, J., Bates, D., DebRoy, S., and R Core Team: nlme: linear and nonlinear mixed effects models. R package version 3.1-149, 2020.

Pitacco, V., Crocetta, F., Orlando-Bonaca, M., Mavrič, B., and Lipej, L.: The Mediterranean stony coral Cladocora caespitosa (Linnaeus, 1767) as habitat provider for molluscs: colony size effect, J. Sea Res., 129, 1–11, https://doi.org/10.1016/j.seares.2017.08.001, 2017.

https://doi.org/10.5194/egusphere-2026-2720
Preprint. Discussion started: 29 May 2026

Pons-Fita, A., Kersting, D. K., and Ballesteros, E.: Co-occurrence of a reef-building coral and canopy-forming macroalgae in the Mediterranean Sea, Mediterr. Mar. Sci., https://doi.org/10.12681/mms.26967, 2021.

Reynaud, S., Leclercq, N., Romaine-Lioud, S., Ferrier-Pagés, C., Jaubert, J., and Gattuso, J.-P.: Interacting effects of CO2 partial pressure and temperature on photosynthesis and calcification in a scleractinian coral, Glob. Change Biol., 9, 1660–1668, https://doi.org/10.1046/j.1365-2486.2003.00678.x, 2003.

Ries, J. B., Cohen, A. L., and McCorkle, D. C.: A nonlinear calcification response to CO2-induced ocean acidification by the coral Oculina arbuscula, Coral Reefs, 29, 661–674, https://doi.org/10.1007/s00338-010-0632-3, 2010.

Ring, S. J., Henehan, M. J., Blukis, R., and von Blanckenburg, F.: Adsorption pathways of boron on clay and their implications for boron cycling on land and in the ocean, Geochim. Cosmochim. Acta, 389, 74–83, https://doi.org/10.1016/j.gca.2024.08.014, 2025.

Rodolfo-Metalpa, R., Martin, S., Ferrier-Pagès, C., and Gattuso, J.-P.: Response of the temperate coral Cladocora caespitosa to mid- and long-term exposure to pCO2 and temperature levels projected for the year 2100 AD, Biogeosciences, 7, 289–300, https://doi.org/10.5194/bg-7-289-2010, 2010.

Ross, C. L., Falter, J. L., and McCulloch, M. T.: Active modulation of the calcifying fluid carbonate chemistry (δ11B, B/Ca) and seasonally invariant coral calcification at sub-tropical limits, Sci. Rep., 7, 13830, https://doi.org/10.1038/s41598-017-14066-9, 2017.

Ross, C. L., DeCarlo, T. M., and McCulloch, M. T.: Environmental and physiochemical controls on coral calcification along a latitudinal temperature gradient in Western Australia, Glob. Change Biol., 25, 431–447, https://doi.org/10.1111/gcb.14488, 2019.

Ross, C. L., Warnes, A., Comeau, S., Cornwall, C. E., Cuttler, M. V. W., Naugle, M., McCulloch, M. T., and Schoepf, V.: Coral calcification mechanisms in a warming ocean and the interactive effects of temperature and light, Commun. Earth Environ., 3, 72, https://doi.org/10.1038/s43247-022-00396-8, 2022.

Royle, S. H., Andrews, J. E., Turner, J., and Kružić, P.: Environmental and diagenetic records from trace elements in the Mediterranean coral Cladocora caespitosa, Palaeogeogr. Palaeoclimatol. Palaeoecol., 440, 734–749, https://doi.org/10.1016/j.palaeo.2015.10.010, 2015a.

Royle, S. H., Andrews, J. E., Marca-Bell, A., Turner, J., and Kružić, P.: Seasonality in sea surface temperatures from δ18O in Cladocora caespitosa: modern Adriatic to late Pleistocene, Gulf of Corinth, J. Quat. Sci., 30, 298–311, https://doi.org/10.1002/jqs.2768, 2015b.

Sadekov, A., Lloyd, N. S., Misra, S., Trotter, J., D'Olivo, J., and McCulloch, M.: Accurate and precise microscale measurements of boron isotope ratios in calcium carbonates using laser ablation multicollector-ICPMS, J. Anal. At. Spectrom., 34, 550–560, https://doi.org/10.1039/C8JA00444G, 2019.

Schiller, C.: Ecology of the symbiotic coral Cladocora caespitosa (L.)(Faviidae, Scleractinia) in the Bay of Piran (Adriatic Sea): II. Energy budget, Mar. Ecol., 14, 221–238, 1993.

Schoepf, V., Jury, C. P., Toonen, R. J., and McCulloch, M. T.: Coral calcification mechanisms facilitate adaptive responses to ocean acidification, Proc. R. Soc. B Biol. Sci., 284, 20172117, https://doi.org/10.1098/rspb.2017.2117, 2017.

Schoepf, V., D'Olivo, J. P., Rigal, C., Jung, E. M. U., and McCulloch, M. T.: Heat stress differentially impacts key calcification mechanisms in reef-building corals, Coral Reefs, 40, 459–471, https://doi.org/10.1007/s00338-020-02038-x, 2021.

https://doi.org/10.5194/egusphere-2026-2720
Preprint. Discussion started: 29 May 2026

Schoepf, V., Sanderson, H., and Larcombe, E.: Coral heat tolerance under variable temperatures: Effects of different variability regimes and past environmental history vs. current exposure, Limnol. Oceanogr., 67, 404–418, https://doi.org/10.1002/lno.12000, 2022.

Schuessler, J. A. and von Blanckenburg, F.: Testing the limits of micro-scale analyses of Si stable isotopes by femtosecond laser ablation multicollector inductively coupled plasma mass spectrometry with application to rock weathering, Spectrochim. Acta Part B At. Spectrosc., 98, 1–18, https://doi.org/10.1016/j.sab.2014.05.002, 2014.

Silenzi, S., Bard, E., Montagna, P., and Antonioli, F.: Isotopic and elemental records in a non-tropical coral (Cladocora caespitosa): Discovery of a new high-resolution climate archive for the Mediterranean Sea, Glob. Planet. Change, 49, 94–120, https://doi.org/10.1016/j.gloplacha.2005.05.005, 2005.

Standish, C. D., Chalk, T. B., Babila, T. L., Milton, J. A., Palmer, M. R., and Foster, G. L.: The effect of matrix interferences on in situ boron isotope analysis by laser ablation multi-collector inductively coupled plasma mass spectrometry, Rapid Commun. Mass Spectrom., 33, 959–968, https://doi.org/10.1002/rcm.8432, 2019.

Stewart, J. A., Anagnostou, E., and Foster, G. L.: An improved boron isotope pH proxy calibration for the deep-sea coral *Desmophyllum dianthus* through sub-sampling of fibrous aragonite, Chem. Geol., 447, 148–160, https://doi.org/10.1016/j.chemgeo.2016.10.029, 2016.

Thil, F., Blamart, D., Assailly, C., Lazareth, C. E., Leblanc, T., Butsher, J., and Douville, E.: Development of laser ablation multi-collector inductively coupled plasma mass spectrometry for boron isotopic measurement in marine biocarbonates: new improvements and application to a modern Porites coral, Rapid Commun. Mass Spectrom., 30, 359–371, https://doi.org/10.1002/rcm.7448, 2016.

Trotter, J., Montagna, P., McCulloch, M., Silenzi, S., Reynaud, S., Mortimer, G., Martin, S., Ferrier-Pagès, C., Gattuso, J.-P., and Rodolfo-Metalpa, R.: Quantifying the pH 'vital effect' in the temperate zooxanthellate coral Cladocora caespitosa: Validation of the boron seawater pH proxy, Earth Planet. Sci. Lett., 303, 163–173, https://doi.org/10.1016/j.epsl.2011.01.030, 2011.

Venables, W. N. and Ripley, B. D.: Modern Applied Statistics with S, 4th ed., Springer, New York, 2002.

Vengosh, A., Kolodny, Y., Starinsky, A., Chivas, A. R., and McCulloch, M. T.: Coprecipitation and isotopic fractionation of boron in modern biogenic carbonates, Geochim. Cosmochim. Acta, 55, 2901–2910, https://doi.org/10.1016/0016-7037(91)90455-E, 1991.

Venn, A. A., Tambutté, E., Holcomb, M., Laurent, J., Allemand, D., and Tambutté, S.: Impact of seawater acidification on pH at the tissue–skeleton interface and calcification in reef corals, Proc. Natl. Acad. Sci., 110, 1634–1639, https://doi.org/10.1073/pnas.1216153110, 2013.

Vergotti, M. J., Kersting, D. K., Comeau, S., Frick, D. A., Hathorne, E. C., Henehan, M. J., Holtz, J., Teixidó, N., van Schijndel, V., and D'Olivo, J. P.: Laser ablation inductively coupled mass spectrometry of trace element composition of a temperate coral Cladocora caespitosa skeleton. GFZ Data, https://doi.org/10.5880/fidgeo.2025.094, 2025a.

Vergotti, M. J., D'Olivo, J. P., Brachert, T. C., Capdevila, P., Garrabou, J., Linares, C., Spreter, P. M., and Kersting, D. K.: Reconstruction of long-term sublethal effects of warming on a temperate coral in a climate change hotspot, J. Anim. Ecol., 94, 125–138, https://doi.org/10.1111/1365-2656.14225, 2025b.

https://doi.org/10.5194/egusphere-2026-2720
Preprint. Discussion started: 29 May 2026

Vergotti, M. J., Kersting, D.-K., Brachert, T., Comeau, S., Frick, D. A., Hathorne, E., Henehan, M., Holtz, J., Teixido, N., van Schijndel, V., and D'Olivo Cordero, J. P.: Data for the research article "High-resolution reconstruction of pH upregulation and its seasonal drivers in the temperate coral Cladocora caespitosa," https://doi.org/10.5281/zenodo.18248853, 2026.

Vogl, J. and Rosner, M.: Production and Certification of a Unique Set of Isotope and Delta Reference Materials for Boron Isotope Determination in Geochemical, Environmental and Industrial Materials, Geostand. Geoanalytical Res., 36, 161–175, https://doi.org/10.1111/j.1751-908X.2011.00136.x, 2012.

Wei, G., McCulloch, M. T., Mortimer, G., Deng, W., and Xie, L.: Evidence for ocean acidification in the Great Barrier Reef of Australia, Geochim. Cosmochim. Acta, 73, 2332–2346, https://doi.org/10.1016/j.gca.2009.02.009, 2009.

Woodhead, J. D., Hellstrom, J., Hergt, J. M., Greig, A., and Maas, R.: Isotopic and Elemental Imaging of Geological Materials by Laser Ablation Inductively Coupled Plasma-Mass Spectrometry, Geostand. Geoanalytical Res., 31, 331–343, https://doi.org/10.1111/j.1751-908X.2007.00104.x, 2007.

Yao, K. M., Marcou, O., Goyet, C., Guglielmi, V., Touratier, F., and Savy, J.-P.: Time variability of the north-western Mediterranean Sea pH over 1995–2011, Mar. Environ. Res., 116, 51–60, https://doi.org/10.1016/j.marenvres.2016.02.016, 2016.

Zeebe, R. E. and Wolf-Gladrow, D.: CO2 in seawater: equilibrium, kinetics, isotopes, Gulf Professional Publishing, 2001.